Technical Report Documentation Page

1. Report No.	2. Government Accession No.	3. Recipient's Catalog No.
FHWA/TX-04/0-4096-1		

4. Title and Subtitle	5. Report Date
Evaluation of Two Monitoring Systems for Significant Bridges in Texas	January 2004
	6. Performing Organization Code

7. Author(s)	8. Performing Organization Report No.
C. T. Bilich and S. L. Wood	Research Report 0-4096-1

9. Performing Organization Name and Address	10. Work Unit No. (TRAIS)
Center for Transportation Research The University of Texas at Austin 3208 Red River, Suite 200 Austin, TX 78705-2650	11. Contract or Grant No. Research Project 0-4096

12. Sponsoring Agency Name and Address	13. Type of Report and Period Covered
Texas Department of Transportation Research and Technology Implementation Office P.O. Box 5080 Austin, TX 78763-5080	Research Report (9/01- 8/03)
	14. Sponsoring Agency Code

15. Supplementary Notes

Project conducted in cooperation with the U.S. Department of Transportation, Federal Highway Administration, and the Texas Department of Transportation

16. Abstract

Two monitoring systems for bridges were evaluated for use by the Texas Department of Transportation. The first system was designed to increase the quantitative information obtained during a routine inspection of a steel bridge. The miniature, battery-powered data acquisition system selected for study has the ability to record a single channel of strain data and use a rainflow counting algorithm to evaluate the raw data. This system was considered to be particularly useful for evaluating fracture critical bridges. The second system provided long-term monitoring of bridge displacements using global positioning systems (GPS). The accuracy threshold of the GPS data was found to be 3 to 4 mm when the data were averaged for 24 hr. Significantly larger errors were observed for shorter averaging durations when satellite coverage was poor. Both monitoring systems are evaluated in this report.

17. Key Words	18. Distribution Statement
bridge monitoring systems, wireless data acquisition, GPS systems, bridge inspection	No restrictions. This document is available to the public through the National Technical Information Service, Springfield, Virginia 22161.

19. Security Classif. (of report)	20. Security Classif. (of this page)	21. No. of pages	22. Price
Unclassified	Unclassified	76	

Form DOT F 1700.7 (8-72) Reproduction of completed page authorized

EVALUATION OF TWO MONITORING SYSTEMS FOR SIGNIFICANT BRIDGES IN TEXAS

by

C. T. Bilich and S. L. Wood

Research Report 0-4096-1

Research Project 0-4096

EVALUATION AND MONITORING OF TEXAS MAJOR AND UNIQUE BRIDGES

conducted for the

Texas Department of Transportation

in cooperation with the

U.S. Department of Transportation
Federal Highway Administration

by the

CENTER FOR TRANSPORTATION RESEARCH
BUREAU OF ENGINEERING RESEARCH
THE UNIVERSITY OF TEXAS AT AUSTIN

January 2004

Research performed in cooperation with the Texas Department of Transportation and the U.S. Department of Transportation, Federal Highway Administration.

ACKNOWLEDGEMENTS

This research project was sponsored by the Texas Department of Transportation (TxDOT) under Project 0-4096. The research team worked closely with Alan Kowalik (BRG), who is thanked for his valuable contributions.

Mezure, Inc. loaned the research team three GPS units, established a website for the project, and assisted the research team in interpreting the results. The assistance of Mike Angus is gratefully acknowledged.

The research team also worked closely with Invocon, Inc. in the refinement of the MicroSAFE devices. Alan Haigood is thanked for his dedication to the project.

The research project was conducted at the Ferguson Structural Engineering Laboratory (FSEL) at the Pickle Research Campus of the University of Texas at Austin. The assistance of laboratory technicians and administrative staff at FSEL was fundamental to the completion of this project.

DISCLAIMER

NOTICE

NOT INTENDED FOR CONSTRUCTION,

PERMIT, OR BIDDING PURPOSES

S. L. Wood, P.E., Texas #83804

Research Supervisor

TABLE OF CONTENTS

LIST OF FIGURES

LIST OF TABLES

SUMMARY

Two monitoring systems for bridges were evaluated for use by the Texas Department of Transportation. The first system was designed to increase the quantitative information obtained during a routine inspection of a steel bridge. The miniature, battery-powered data acquisition system selected for study has the ability to record a single channel of strain data and use a rainflow counting algorithm to evaluate the raw data. This system was considered to be particularly useful for evaluating fracture critical bridges. The second system provided long-term monitoring of bridge displacements using global positioning systems (GPS). The accuracy threshold of the GPS data was found to be 3 to 4 mm when the data were averaged for 24 hr. Significantly larger errors were observed for shorter averaging durations when satellite coverage was poor. Both monitoring systems are evaluated in this report.

CHAPTER 1:
INTRODUCTION

Within the past twenty-five years, several important bridges have been constructed within the State of Texas which utilize relatively uncommon structural systems, such as cable-stayed superstructures or post-tensioned box girders. Because of their unique designs, the Texas Department of Transportation (TxDOT) is concerned that the structural response of these bridges may be different than the vast majority of bridges in the state and that standard inspection techniques may not be sufficient to detect the onset of structural damage. TxDOT project 0-4096, Structural Health Evaluation and Monitoring of Major and Unique Bridges in Texas, was funded to identify and evaluate monitoring technologies that could provide information about the behavior of these unique bridges that is not available during routine inspections.

This report summarizes the progress that has been made during the first two years of this project. Two monitoring technologies are evaluated. One system is designed to be installed easily in the field, provide enhanced information to TxDOT personnel during an inspection, and then be moved to another structure. The advantages of this monitoring system include the size of the data acquisition system and the user interface. Rainflow data are available immediately to the inspection team and can be used directly to evaluate the fatigue life of the bridge. The research team worked closely with the developer of this monitoring system during the project, and several refinements were made. Field implementation tests are scheduled to begin in early 2004.

The second monitoring system is designed to identify changes in the long-term response of a bridge. Data from this system are collected and interpreted by an independent company. The advantages of this monitoring system include easy access to the data by engineers within the Bridge Division and the independent company retains responsibility for maintenance of the system. Testing of this second system was terminated prematurely when the company providing the equipment filed for bankruptcy. Other companies provide similar monitoring services; therefore, the evaluation of the technology is not limited to this one service provider.

1.1 RECENT EXPERIENCES BY TXDOT

The research team is aware of two monitoring efforts by TxDOT within the last several years: acoustic monitoring of the stay cables on the Fred Hartman Bridge and scour morning of the bridge piers on FM 1157 over Mustang Creek. Monitoring of the Fred Hartman Bridge by Pure Technologies, Inc. is considered to be a success. Staff from Pure Technologies installed three accelerometers on each of the 192 stay cables and monitors the response of each instrument for indications of damage. To date, the system has detected a number of events. Weld fractures of the guide pipes have been confirmed and possible wire breaks have been identified. Pure Technologies is responsible for maintaining the monitoring system and evaluating all data. All information is available to TxDOT personnel via a secure web site.

The scour monitoring system was not as successful. The system was developed during a research project, and was not ruggedized for field use. In addition, TxDOT district personnel were responsible for maintaining the system and interpreting the data. Therefore, training of field personnel became an important concern and data were often not available for evaluation by engineers in the design division. As a result of these technical and administrative problems, TxDOT currently relies on underwater inspection, rather than a scour monitoring system, to identify possible structural problems.

Based on these experiences, TxDOT suggested that the research team not investigate monitoring technologies that must be maintained by district personnel or that required special training to interpret the data. The two systems discussed in this report satisfy these requirements. In one case, the algorithms needed to convert the raw data into engineering data are programmed into the data acquisition systems,

and engineering (rainflow) data are reported directly. In the other case, an independent organization interprets the data and notifies TxDOT of changes to long-term trends which indicate structural damage.

1.2 SURVEY OF CURRENT PRACTICES IN THE US

To evaluate current practices in the US related to structural health monitoring of bridges, the research team surveyed all state Departments of Transportation. The results of this survey are summarized in this section.

The Florida Department of Transportation uses global positioning (GPS) technology to monitor structural displacements on the Dames Point Bridge, a 1300-ft concrete, cable-stayed span over the St. John's River in Jacksonville. Five points on the structure are monitored using GPS hardware and services provided by Mezure, Inc. This GPS technology provides an automated system that facilitates the full-time, long-term monitoring of structural displacements without regular attention or maintenance (Angus, 2001).

The Alabama DOT has developed and tested two systems that monitor bridge scour. The first system, installed on two bridges, uses a modified depth finder. This system sends alerts via cellular signal when a scour problem is detected. The second system uses tilt meters on the bridge to monitor pier movement due to scour. Both of these systems operate autonomously during data acquisition. However, the systems were developed by researchers and require regular attention by AlDOT personnel for maintenance and upkeep (Conner and Conway, 2001).

The Connecticut DOT, in conjunction with the University of Connecticut, has developed extensive systems to monitor various aspects of structural performance on almost any bridge. These systems use tilt meters, accelerometers, displacement gages, and strain gages. These complex systems are bulky and are not durable in a long-term outdoor environment. Data can be acquired autonomously, but complex data reduction algorithms are required to obtain meaningful engineering data (Sime and D'Attilio, 2001).

The Delaware DOT has installed permanent monitoring systems on three bridges, each acquiring a variety of data (strains, loads, deflections, tilt angles, accelerations). DelDOT is experimenting with compact, battery powered, rapidly deployable data acquisition systems for strain measurement of bridges girders and decks. The current generation of hardware requires the data to be downloaded each month. Future generations will have the ability to send strain data over the Internet. All DelDOT systems acquire raw data that must then be analyzed by DelDOT personnel before meaningful engineering values are obtained (O'Shea, 2001).

The Kentucky DOT performs short-term monitoring on problem bridges only. This involves the use of strain gages, acoustic emission, and occasional video setups. Similarly to the data acquisition systems used in Connecticut, these systems are complex, bulky, and not durable in a long-term outdoor environment (Givan, 2001).

The New York DOT has not implemented any systems that monitor a bridge as a whole, but has funded research to establish long-term monitoring systems. According to the NYDOT, baseline information must include data from complete environmental cycles because measurements vary considerably with temperature, solar radiation, and vehicular traffic (Alampalli, 1999). Also, changes in modal frequencies and mode shapes have been used to evaluate bridge damage (Alampalli, 1995). However, these techniques still rely on researchers for implementation and evaluation of data.

Other states described activities with goals and objectives similar to those for this project, but had not implemented real-time monitoring to date. Many states continue to use visual inspections as the only indicator of overall structural health. Inspectors visually examine key structural components for signs of damage. If damage is detected, repairs are performed and the bridge remains in service.

1.3 SCOPE OF PROJECT

Based on recent experiences at TxDOT, the research team decided to investigate two types of monitoring systems.

The first system selected for evaluation was designed to enhance the amount of quantitative information that is available during routine inspections of bridges. This battery powered, self-contained, miniature data acquisition system, developed by Invocon, Inc., can be easily installed in the field and provides the inspection team with rainflow counting data, in addition to raw strain data. The ability to acquire actual strain data would be especially important for inspection of fracture-critical bridges.

A GPS-based system for monitoring structural deformations was selected because the conceptual design of the system is similar to the monitoring system that has been installed on the Fred Hartman Bridge. The GPS units are purchased from the company that will install the units. For an annual fee, this company is responsible for interpreting the data and maintaining the units. The GPS system developed by Mezure, Inc. was selected for investigation because of the experiences working with the Florida DOT and because the web-based interface provided an easy way to obtain and interpret the data.

The experiments used to evaluate the two monitoring systems are presented in this report. Chapter 2 discusses the strain-recording system by Invocon, as well as the collection and evaluation of data from this system. Chapter 3 presents a brief history of satellite navigation systems and discusses the Mezure system used for monitoring structural deformations. Chapter 4 discusses the collection and evaluation of data from the Mezure system. Chapter 5 presents conclusions and recommendations for future research.

CHAPTER 2:
AUTONOMOUS DATA ACQUISITION SYSTEM FOR STRAIN

Over the past twenty years, a large number of researchers have measured the response of bridges in the field and then analyzed the data to evaluate the condition of the bridge. While this method of operation has proven to be effective in the research environment, the data acquisition systems and data reduction algorithms are not well suited to the needs of a Department of Transportation which must inspect all bridges on a bi-annual basis. The data acquisition system described in this chapter was designed specifically for these frequent inspections.

Each data acquisition unit is battery powered, small enough to sit on the bottom flange of a steel girder, and records data from a single, 120-Ω strain gage. Perhaps most importantly, the unit has been designed to generate rainflow counts directly, so that the inspection team can evaluate the strain ranges experienced at a given location on the bridge rather than analyzing thousands of points of strain data. The research team believes that there are many applications for this type of autonomous data acquisition system.

This Chapter is divided into three sections. The ASTM E 1049-85 rainflow counting algorithm is briefly described in Section 2.1. An overview of the features of the data acquisition system is given in Section 2.2, and the system is evaluated critically in Section 2.3.

2.1 RAINFLOW COUNTING

Rainflow counting is a method of simplifying a complex strain history into a histogram of cycle amplitudes. By counting the number of times that a structure experiences cycles of a given level of strain, the likelihood of fatigue damage and the remaining fatigue life can be predicted (Downing and Socie, 1982).

The rainflow counting algorithm is described using the sample loading history shown in Figure 2.1, which was taken from the ASTM E 1049 specification for rainflow counting. The loading units in this sample history can be assumed to be directly proportional to both stress and strain in the specimen.

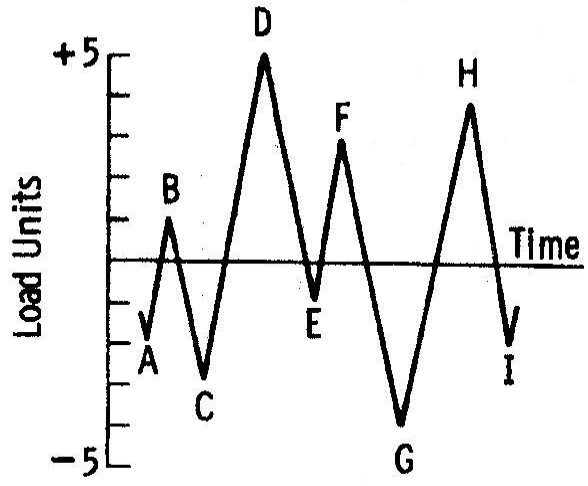

Figure 2.1: Example Loading History (ASTM E 1049)

The ASTM algorithm for rainflow counting may be used to evaluate previously recorded data, as well as strain histories that are measured, counted, and discarded in real time. The strain history is examined point-by-point, beginning with the first observed data point. A simple series of Boolean checks are performed to compare the current strain with the adjacent maximum and minimum strains in the history. In this manner, the number of cycles within predetermined ranges of strain are calculated.

The strain history shown in Figure 2.1 can be reduced into the cycle counts presented in Table 2.1 using the rainflow counting algorithm. Because each of the relative maxima and minima in this example corresponds to an integer value of strain, the stress ranges in Table 2.1 are also expressed as integer values.

When actual data are acquired in a realistic environment, many cycles are recorded in a given strain history and recorded values of strain are not integers. If this rainflow counting algorithm were used with actual data, an extensive table of stress ranges, each likely to have only a single or half-cycle, would be generated. These data would be voluminous and difficult to interpret.

Range bins allow the individual cycles to be combined into more meaningful groups. An example of binned data is shown in Table 2.2. The size of each range bin is 3 units. Cycles from 0 to 3 units are counted in the first bin, cycles from 3 to 6 units are counted in the second bin, and cycles from 6 to 9 units are counted in the third bin. Cycles falling on the edge of a bin (stress range of 3, for example) can be counted in either bin at the discretion of the rainflow algorithm programmer. The resulting table (Table 2.2) is a more condensed version of Table 2.1, where data are easier to interpret and more meaningful in fatigue life analysis.

Table 2.1: Rainflow Cycle Counts for ASTM Example

Stress Range (units)	Cycle Counts	Events
1	0	
2	0	
3	0.5	A-B
4	1.5	B-C, E-F
5	0	
6	0.5	H-I
7	0	
8	1.0	C-D, G-H
9	0.5	D-G
10	0	

Table 2.2: Binned Cycle Counts for ASTM Example

Range Bin (units)	Cycle Counts	Events
0-3	0.5	A-B
3-6	2.0	B-C, E-F, H-I
6-9	1.5	C-D, G-H, D-G

2.2 THE MICROSAFE SYSTEM

This section describes the features of a commercially available, autonomous strain recording device called MicroSAFE. MicroSAFE stands for "Micro-miniature Stress Analysis and Forecasted Endurance," and was developed by Invocon, Inc., located in Conroe, Texas.

2.2.1 Background

MicroSAFE is a single-channel data acquisition system intended to aid in fatigue life estimation of structural elements. Invocon began development of this technology for the National Aeronautics and Space Administration (NASA) in the late 1990's. Early versions recorded raw strain data on the space shuttle for analysis upon mission completion. These devices would monitor and record strains within the structural components of the space shuttle during launches and landings. Upon return to earth, the devices would be removed, and the data would be downloaded and analyzed. These data were used to determine the amount of fatigue damage done on each mission and predict the remaining amount of service life for each shuttle.

2.2.2 First Generation

In 2000, researchers at the University of Texas at Austin began working with Invocon to build a series of similar devices that could be used to monitor bridges. A photograph of the first device is shown in Figure 2.2. The unit measured 1.2 in. x 1.2 in. x 0.6 in. The system could record data at 7.1 Hz and compute rainflow counts as the data were acquired. An internal battery with an expected life of 36 hours provided power. Once programmed for acquisition, the system was 100% autonomous.

Figure 2.2: First Generation MicroSAFE Device

Limited testing was done using this device. Available battery power and data acquisition speed were deemed to be the limiting factors for bridge applications. Also, this unit was not enclosed in a weatherproof container.

2.2.3 Second Generation

The research described in this report began using the second generation of the MicroSAFE devices. Invocon delivered eleven second-generation units to the University of Texas in late 2001, along with an updated software package that facilitated the programming of this generation of devices. Over the next 2 years, Invocon worked closely with the research team to test, evaluate, and update the devices.

This generation of devices was designed to be weatherproof. Each device was potted using epoxy material and used weatherproof rubber connectors. Power was provided by an external, non-rechargeable battery pack, which also was encased in epoxy potting material and weatherproof connectors. This battery pack was designed to power a single MicroSAFE unit for three months of continuous data acquisition, removing battery life as the limiting factor for monitoring applications. Figure 2.3 shows the battery pack (larger device on left) connected to the MicroSAFE hardware (smaller device on right).

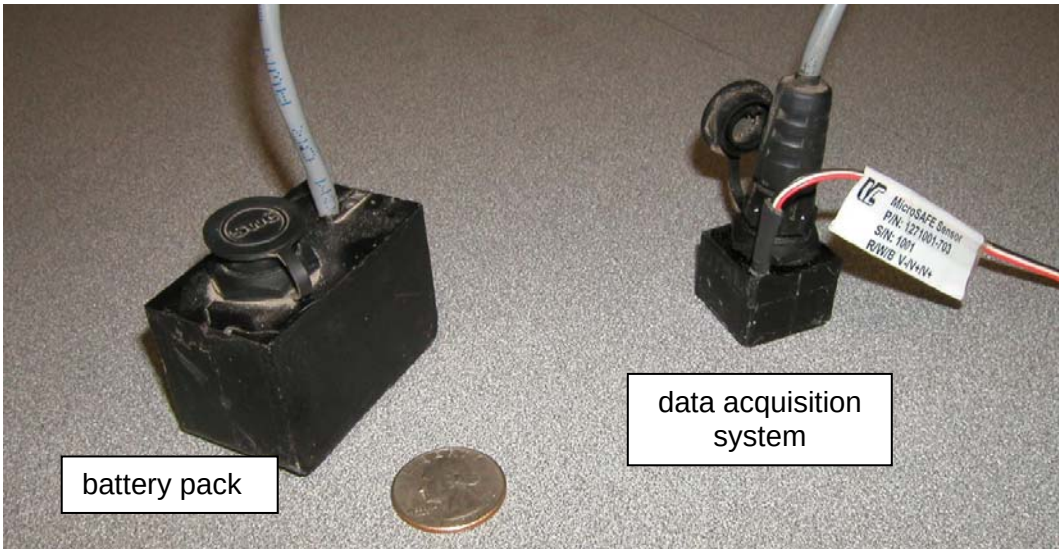

Figure 2.3: MicroSAFE Battery Pack and Hardware

An updated graphical user interface (GUI) was provided with this generation of MicroSAFE devices. The GUI is a computer program that is used to communicate with the MicroSAFE devices, program them for data acquisition, download data sets when the unit has completed data acquisition, and view downloaded data sets graphically in a variety of ways.

During the programming of the unit for data acquisition, various options are available. These options include the type of data acquisition, data acquisition mode, gage factor, data sampling rate, and bin size for rainflow analysis. The user can select the start and stop times for data acquisition, the number of consecutive data acquisition cycles, and the time between cycles.

Data acquisition can be started by setting a specific time or by an event-detection mode. In the event-detection mode, the unit would power off and "sleep" for a user-determined amount of time. It would then power on, "wake up," and monitor the strain gage for an event where strains were larger than a user-set threshold value. If the strain event contained strains over the threshold value, the unit would acquire the desired amount of data (number of cycles, length of data acquisition, etc.) before powering off and starting the process over. If the strain event did not cross the threshold value, the unit would power off and wait for the next time when it would power on and monitor the gage again. This function was intended to allow very long periods of observation where insignificant strain events (those below the threshold value) would not be recorded, preserving both battery life and available memory.

Because of the speed of traffic on in-service bridges, a single strain gage would most likely only experience an extreme strain event (a large truck crossing the bridge) for a few seconds. The odds of this event being observed within the brief event-detection window are small. If the event did happen to be captured in the event-detection window, the duration of the event would not be long enough to be captured once the unit has powered on and started to record data. For these reasons, the event-detection mode did not seem practical for monitoring strain events on a bridge and will be removed in future versions of the GUI.

A variety of data could be captured with this second-generation device. These included raw strain data capture only, raw data capture and immediate, onboard rainflow counting of this data, and rainflow counting only. During the "rainflow counting only" acquisition mode, no raw data were saved in memory. The option for raw data capture would allow the user to perform a variety of analyses following data capture, while the rainflow option would allow the user to see how the structural element was performing immediately after data capture. The "raw and rainflow" option allowed the user to have both a rainflow count for the recorded strain history and the raw strain data from which the rainflow count was obtained. Any time raw data are captured, available memory on the MicroSAFE device becomes the limiting factor in data acquisition time.

The data rate could be specified to be 8, 16, or 32 Hz. At the maximum data acquisition rate, available memory would be fully utilized after only 34 min of continuous data acquisition. This was viewed as a limitation to the MicroSAFE devices and may be addressed in the next generations.

Data acquisition time is also limited to 34 min per cycle while taking rainflow data only. Although the available memory will be only 1.2% full with a single 34-min rainflow-only cycle, the maximum rainflow acquisition time per cycle was still limited by the GUI. If more than one sampling cycle was requested, the MicroSAFE unit would have to sleep for 8 sec to log the rainflow counts to a data file before beginning the next cycle. After downloading the completed rainflow data, each cycle would be represented in a separate data file.

If the user wished to observe the behavior of a structural component over a 24-hr period, 48 30-min cycles would have to be programmed. Following download, all 48 sets of rainflow cycle counts would need to be combined to get a clear picture of how the structural component behaved for that 24-hr period. In February 2003, Invocon released a Rainflow Combining Utility that allowed the graphical viewing of multiple rainflow files at one time, and the combination of the values found in each bin of these files. Although the addition of this program allowed the creation of 24 hr of continuous sampling, these extra steps proved to be confusing and difficult. These concerns were addressed in the next version of the GUI and will be described in depth in the following section.

The majority of tests discussed in the following sections of this chapter were performed using MicroSAFE devices from the second generation. As testing progressed, communication between the research team and Invocon produced five new versions of the GUI (versions v2.0 through v2.4), each more refined than the previous version. MicroSAFE hardware remained the same throughout these tests.

2.2.4 Third Generation

In early 2003, the Invocon discovered a problem with the manner in which individual rainflow counts were assigned to bins during data acquisition. This scheme was hard-coded within the MicroSAFE devices and could not be reprogrammed. All eleven devices were returned to Invocon in March 2003, for repair. Invocon replaced the non-programmable internal hardware with programmable chips and returned the units. Functionality of the units remained the same between generations, but the identified errors were corrected. This marked the beginning of the third and final hardware generation. Limited testing was done using this generation, and will be discussed later in this chapter.

Following the return of the third generation of devices, the research team discovered an error in the rainflow counting algorithm. This error had been present in all previous generations of the MicroSAFE product. In May 2003, Invocon rewrote the rainflow counting algorithm. The units were returned to Invocon in July 2003 for reprogramming, and the improved units were returned to the research team in October 2003.

2.3 MICROSAFE EVALUATION

To evaluate the MicroSAFE system and determine if TxDOT could use the units effectively, the research team tested the units in a variety of environments. First, the accuracy of recorded strains was verified in a laboratory environment. Next, raw data and rainflow recording abilities were tested in a field environment. The durability of the hardware was tested in a corrosive, outdoor environment. Finally, rainflow recording abilities were further tested in a laboratory environment.

2.3.1 Verification of Data Acquisition

The first step in evaluating the MicroSAFE system was to verify the accuracy of the raw strain data recorded by the units. As stated previously, MicroSAFE can record raw strain data and perform onboard rainflow counting as data are taken. It can be assumed that accurate rainflow counts cannot be obtained without accurate strain data. Therefore, it was necessary to verify the accuracy of the recorded strains before proceeding with further testing.

A Measurements Group 1550A Strain Indicator Calibrator was used to produce simulated strains that could be recorded by the MicroSAFE device. Before using the 1550A as a strain benchmark, it was checked for output accuracy using a Measurements Groups P-350A Strain Indicator. Strains of various magnitudes were simulated using the 1550A calibrator. These strains ranged from 100 με to 4,000 με. The results are summarized in Table 2.3.

Table 2.3: Strain Indicator Calibrator Verification

Strain Calibrator (με)	Strain Indicator (με)	Percent Error
100	100	0%
200	200	0%
300	300	0%
400	400	0%
1000	999	0.10%
2000	2001	0.05%
3000	3003	0.10%
4000	4009	0.23%

The percent error of the 1550A calibrator increased slightly as simulated strain increased. The maximum error level was 0.23% at 4,000 με. This level of strain corresponds to approximately 138 ksi of stress in structural steel (assuming the steel does not yield), and exceeds the maximum tensile stress that would be resisted by any structural steel shape (AISC 1998).

Four of the eleven MicroSAFE units were selected at random for strain verification using the 1550A calibrator. Units were tested one at a time, recording strain data for 30 sec as the calibrator was cycled

through each of the eight strain levels listed in Table 2.3. Each strain was held for approximately 3 sec. The recorded strain values were then compared with the input strain values. Results of the four tests are summarized in Table 2.4.

Table 2.4: MicroSAFE Strain Verification

Strain Indicator (με)	Recorded Strain (με) for Each Unit				Average Percent Error
	#1000	#1001	#1003	#1005	
100	101	100	100	100	0.3%
200	199	201	200	198	-0.3%
300	299	302	300	299	0.0%
400	394	402	400	399	-0.3%
999	998	1004	1000	997	0.1%
2001	1998	2005	2000	1998	0.0%
3003	2998	3006	3000	2996	-0.1%
4009	3998	4008	3999	3993	-0.2%
				Average	**-0.1%**

Individual recorded strains were within 1.0% of the corresponding input strain. When errors corresponding to a single strain value were averaged for all four units, maximum error was reduced to 0.3%. From this examination, it can be concluded that the MicroSAFE devices would record sufficiently accurate strain data for strains up to 4,000 με.

During the recording of a static strain, a certain level of background noise is recorded by each MicroSAFE device. This level varies from unit to unit, peaking at 10 με and averaging 3 - 4 με. A 3-sec history as a constant input strain is shown in Figure 2.4. This strain history would produce rainflow cycle counts with magnitudes ranging from 0 - 8 με due to background noise, which would saturate the smallest bin(s) in the rainflow histogram. Bins of larger magnitude than the observed background noise would continue to contain reliable counts.

This background noise cannot be removed from the strain history or the rainflow results. For this reason, the new GUI will include a function that will ignore cycles with magnitudes lower than a threshold value specified by the user. These cycle counts will be removed from the rainflow histogram so that it will more accurately represent the number of cycle counts at lower strain ranges. The discarded cycle counts will be logged in the full data file for retrieval upon demand.

Background noise is present at all times during strain measurement. The magnitude of the background noise is random, but remains small in comparison to the magnitudes of strain cycles that will affect the fatigue life of a steel structure. Therefore, the level of background noise present in the MicroSAFE strain measurement will not adversely affect fatigue life predictions using this system.

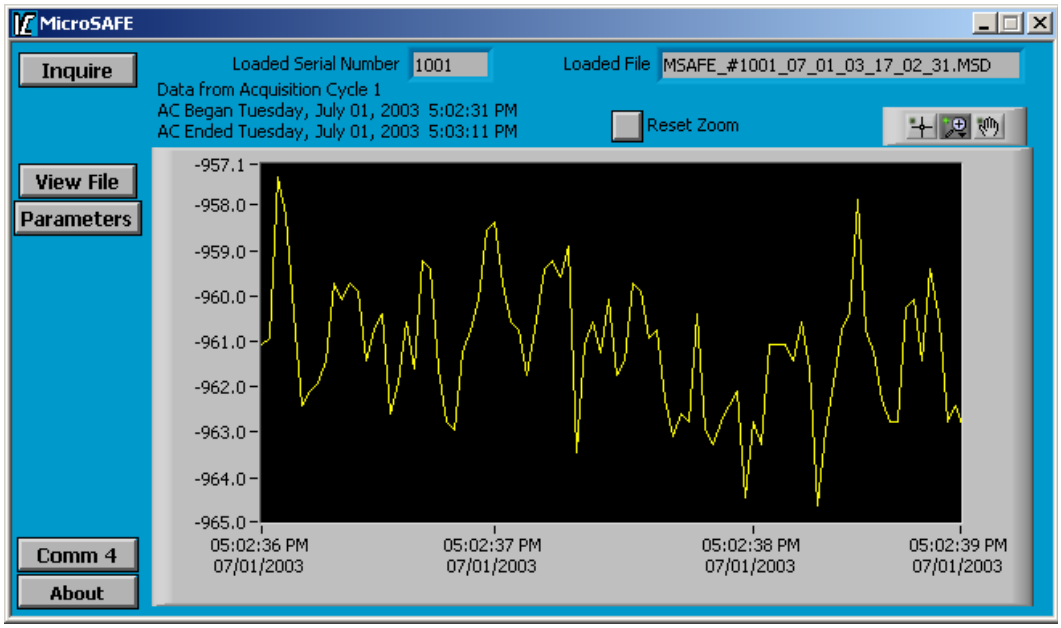

Figure 2.4: MicroSAFE Background Noise Sample

2.3.2 Field Testing on US 183/Texas 71 Bridge

Field-testing of the MicroSAFE units was performed near Austin, Texas, on the bridge that carries westbound Texas State Highway 71 over US Highway 183 (Figure 2.5). This structure was selected because the layout permitted access to the girders at midspan of the center span without obstructing traffic.

The TX 71/US 183 overpass is a 6-girder steel bridge with a concrete deck. Steel girders are continuous over pinned supports at the concrete bent caps. The concrete deck acts compositely with the steel girders over five spans. All testing was performed at midspan of the center span.

Ten MicroSAFE units were tested in this field study. Units were mounted on the top face of the bottom flange of the interior girders. Placement on the lower flanges of interior girders at midspan ensured the highest possible tensile strain signals during traffic loading. The units were arranged in five pairs. Strain gages in each pair were arranged in a nose-to-nose fashion, as shown in Figure 2.6.

Figure 2.7 shows a pair of MicroSAFE units installed on the bridge. All gage pairs were installed with identical configurations. Because both gages in a given pair were positioned in almost identical locations on the structure, this configuration allowed a pair of MicroSAFE units to record identical strain data simultaneously in the field. Figures 2.9 through 2.12 contain plots of the measured data. These figures show nearly identical strain histories when corrected for minor initial strain and time differences between MicroSAFE units. These corrections are discussed later in this section.

Figure 2.5: Texas 71/US 183 Overpass

Figure 2.6: Placement of Pairs of Strain Gages

Figure 2.7: MicroSAFE Units Paired on Bridge

Testing on the TX 71/US 183 overpass lasted approximately one year. Over this period, the units were acquiring data approximately 10-20% of the time. Performance and durability of the units were very good. More than 200 acquisition sequences were programmed during field testing. The units acquired the appropriate data in approximately 97% of the sequences. In one case, there were no data present on the MicroSAFE device following acquisition. In two cases (on two different MicroSAFE units), data were present on the unit but download was not possible. Following reprogramming, each unit performed normally for the duration of its service. In another case, one unit would acquire strain data, but returned zero cycle counts when programmed to take rainflow data. This was later traced to an internal programming error in the auto-zero function within that particular MicroSAFE device. The unit was reprogrammed by Invocon and has been functioning normally since.

The units were programmed to acquire both raw strain data and rainflow data an acquisition rate of 32 Hz for most of these tests. A few tests were performed using acquisition rates of 8 or 16 Hz. As expected, the peaks and valleys were less pronounced in the strain histories when the data were captured at the slower data acquisition rates. As a result, acquisition rates for all subsequent tests were set at 32 Hz.

Each round of tests was conducted by programming all 10 units to perform the same type of data acquisition using the same bin size. Bin sizes were varied between tests, starting at 10 με and increasing by 10 με for each successive round of testing. When bin size reached 50 με, all observed stress ranges were being logged in the first half of the bins. The maximum bin resolution was no longer being used. Bins were therefore limited to 50 με.

Acquisition periods for these tests were set at the maximum of 34 min. As stated previously, 34 min of continuous raw strain and rainflow data recorded at 32 Hz filled the available memory completely. The maximum acquisition time was employed to acquire the maximum number of strain cycles during an acquisition, helping to test the rainflow counting algorithm. However, even when using the maximum acquisition time of 34 min, most of the bins in the rainflow histogram contained zero cycles. There were not enough high strain cycles occurring within the 34-min acquisition window to populate all bins. Longer rainflow acquisition times would likely capture a few cycles of higher strain, however it was not possible to record raw strain data during the longer acquisition windows.

In an attempt to collect data over a longer duration, the same series of tests were performed again (using maximum acquisition time and varying bin sizes for each round of tests), but the start times for the five gage pairs were staggered so that acquisitions could be performed sequentially. Approximately 2.5 hr of continuous raw strain and rainflow data could now be acquired on the structure. Although each gage pair

was not positioned at exactly the same location on the structure, the technique was successful in creating a combined, continuous raw strain history and a corresponding set of rainflow counts.

An interesting observation was made during field-testing on the TX 71/U.S. 183 overpass. When two MicroSAFE units were programmed to begin identical acquisitions at the same time, small timing discrepancies between the two units were observed. This discrepancy results from the manner in which time is kept on each MicroSAFE unit.

When a unit is programmed for acquisition, the internal clock on the MicroSAFE device is synchronized to the computer clock. The clock speeds of the microprocessors within each MicroSAFE unit are used to count time once an acquisition has been programmed. Due to variability in the manufacturing of the microprocessors, the clock speed of each unit is slightly different. Therefore, there will be a minor time mismatch among the MicroSAFE units that cannot be removed. This mismatch will not vary more than a few seconds during a given acquisition (Haigood, 2002).

These effects can best be seen in Figures 2.9 through 2.12. MicroSAFE units #1001 and #1004 were programmed to take both raw strain data and rainflow data beginning at the same time. Raw strain data versus the time since the start of data acquisition (according to each unit) are plotted in these figures. Near the start of the acquisition period (approximately 108 sec into the 2000-sec acquisition period) the data series recorded by unit #1004 had to be shifted left by 0.27 sec to overlap the data series recorded by unit #1001, as shown in Figure 2.8. This value was called a *time offset*, because it represents the time shift between two units due to different clock speeds.

Near the end of the acquisition period (Figure 2.11, at approximately 1536 sec into the 2000-sec acquisition), 2.0 sec of adjustment was required to produce overlap in the data series. By computing time offsets at other points between 0 and 2000 sec, shown in Figures 2.10 and 2.11, the offset was found to vary linearly with time. These results, shown in Table 2.5, were expected because the time offset is due to differences in the clock speed between the microprocessors.

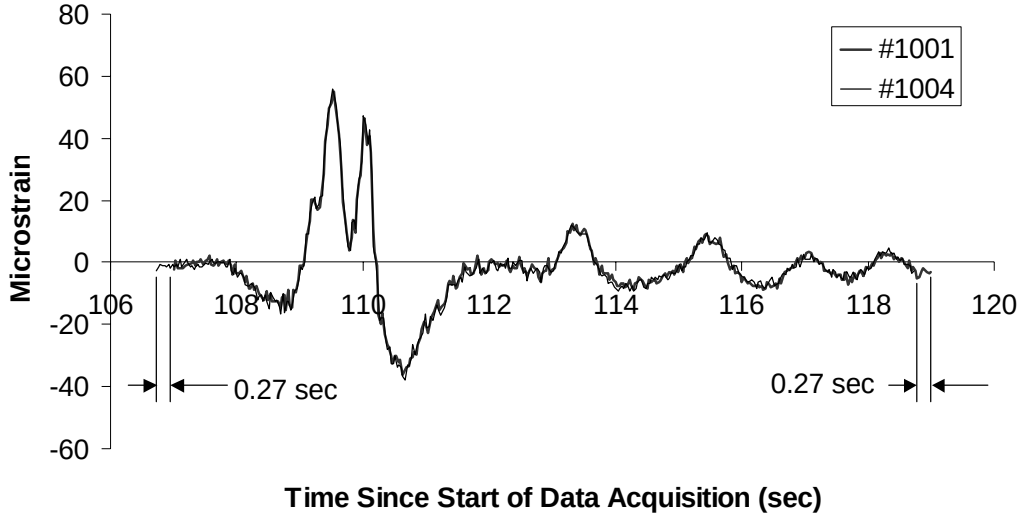

Figure 2.8: Corrected Strain vs. Time Approximately Two Minutes into Acquisition Period

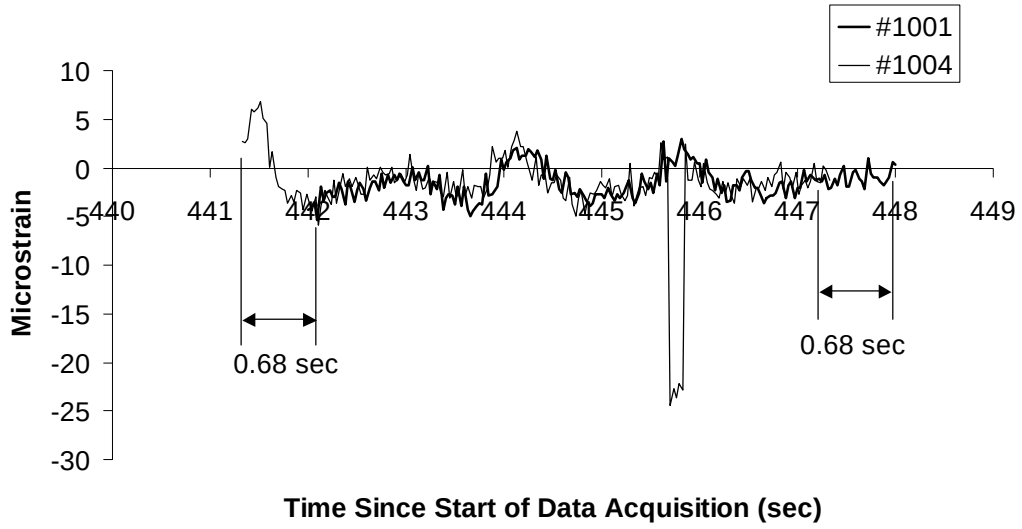

Figure 2.9: Corrected Strain vs. Time Approximately 7.5 Minutes into Acquisition Period

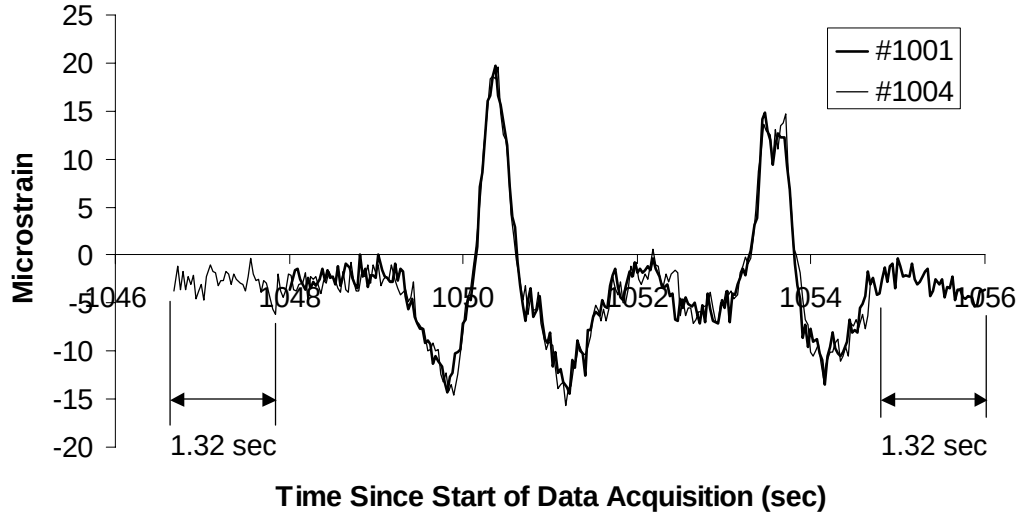

Figure 2.10: Corrected Strain vs. Time Approximately 17.5 Minutes into Acquisition Period

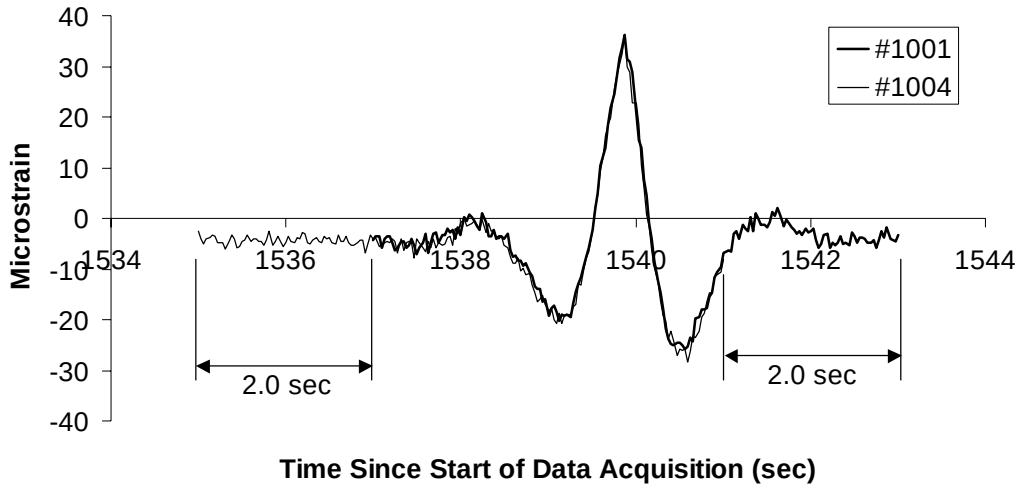

Figure 2.11: Corrected Strain vs. Time Approximately 25.5 Minutes into Acquisition Period

Table 2.5: Strain and Time Offset Values

Time (sec)	Time Offset (sec)	Strain Offset (με)
108	-0.27	-1.5
442	-0.68	-1.0
1048	-1.32	-3.0
1536	-2.0	-5.0

Strain offsets were also observed at various times between 0 and 2000 sec. These values were used to correct the strain values and produce agreement in the data series. They are listed in Table 2.5, as well. Strain offsets were found to be generally increasing with time, but they did not increase linearly. It is most likely that these variations in strain between data sets are caused by background noise.

When both strain and time offsets are considered, Figures 2.9 through 2.12 show that data agreement between the two MicroSAFE devices is very good. Small variations (2 – 3 με) between the two devices are visible at times due to background noise. However, overall, the strain histories are so similar that it is difficult to distinguish one from another.

Figure 2.9 shows a brief but significant disturbance in the strain history for unit #1004. The cause of this disturbance is unknown. However, this was the only signal disturbance recorded during field testing that was not attributed to background noise.

Regardless of the cause of the time and strain offsets, they should not adversely affect acquisition of raw strain data or the corresponding rainflow data.

2.3.3 Durability Testing on Fred Hartman Bridge

To test the durability of the MicroSAFE system in a corrosive environment, a single MicroSAFE unit was installed at the center of the main span of the Fred Hartman Bridge. This bridge (Figure 2.12) spans the Houston Ship Channel between Baytown and LaPorte, Texas. The environment in this area is known for being highly corrosive and was, therefore, selected for this durability study.

Figure 2.12: Fred Hartman Bridge (TexasFreeway.com, 2003)

The duration of the study was one month. The MicroSAFE unit tested in this study was provided and managed by Invocon for the duration of the study.

Various acquisitions were programmed during this month. According to Invocon, the unit performed flawlessly during all acquisitions. The physical condition of the unit following the study was also very good.

Figure 2.13 shows the unit installed on the Fred Hartman Bridge. The battery shown in this figure is a prototype of the new battery pack, where individual cells can be replaced without replacing the entire battery pack structure. According to Invocon, this battery pack performed as expected during the month of acquisitions. No special attention was required during acquisition. Upon removal and inspection, there was no evidence of corrosion within the battery pack.

2.3.4 Milling Machine Tests

It was also desired to verify the accuracy of the rainflow counting algorithm for each unit. An apparatus was devised that would reproduce a given strain history an arbitrary number of times. This would allow identical strain signals to be sent to any number of MicroSAFE devices. The return of identical rainflow counts between units would then verify that all MicroSAFE devices were retrieving the same data and performing identical operations.

A 1” x 12” x 1/8” aluminum bar was chosen as the test specimen for these tests. The bar was attached to the surface of a computer numeric controlled (CNC) milling machine. Figure 2.14 shows the test bar and the CNC milling machine. The right end of the bar was clamped to the milling surface (not shown in Figure 2.15). The left end was pressed between a double-roller support, used to eliminate localized moments at the free end of the beam. The double-roller was then fixed in the stationary head of the milling machine. As the milling surface was displaced by computer control, relative displacements between the ends of the bar were induced. This arrangement created a cantilevered beam with a clear span of 10”.

The CNC milling machine could be programmed to displace the milling surface with respect to the fixed head at up to 45 in./min. At this speed, actual displacements of the milling surface would be within

0.001” of the programmed displacement. The displacement scheme generated strains in the cantilevered bar, which were recorded by the MicroSAFE units.

Figure 2.13: MicroSAFE Unit on Fred Hartman Bridge

Figure 2.14: Test Beam on CNC Milling Machine

Two strain gages were mounted on the bar, one on each side. Both gages were located 1" from the fixed end, where high strains were expected. Terminal blocks were attached to each strain gage to facilitate easy attachment of the MicroSAFE lead wires.

During a given test, one side of the beam is in compression while the other is in tension. Because the cross section of the beam is symmetric, and both gages were placed at the same distance from the fixed end, the absolute values of the strain magnitudes experienced by each gage would be identical. The signs of the strains would, however, be reversed. Although mirror-image strain histories would be observed when both gages are acquiring data simultaneously, rainflow counts for these histories would be identical. This hypothesis was verified during testing. MicroSAFE units recording data simultaneously produced identical rainflow counts.

Six MicroSAFE units were chosen at random for this test. The first three tests were performed with units #1006 and #1007, adjusting bin sizes between each test until proper bin sizes were selected. Following this, four additional MicroSAFE units were selected and tested. All six units sampled the strain history shown in Figure 2.15. From this strain history, each unit produced an identical rainflow count. A representative rainflow count is shown in Figure 2.16. These tests proved that the rainflow counting algorithms on each MicroSAFE unit worked identically.

Because of the background noise effects discussed in Section 2.3.1, the first bin in the rainflow cycle count table becomes saturated relative to the number of counts in the remaining bins. Though the MicroSAFE GUI enabled the user to change the values on both the X- and Y-axis, effectively scaling the plot into any desired window, not all data analysis will be done using the GUI. Therefore, when plotting the rainflow data as they are stored, the saturated bin will affect the visibility of counts in the other bins, as shown in Figure 2.16

Figure 2.17 shows the same rainflow cycle counts, but with the background noise removed from the first bin. All cycles less than 8 με in magnitude were removed from the first bin, using a simulation of the new GUI that was released in October 2003. As a result, the plot is rescaled and the data in the larger bins become easier to interpret and more meaningful.

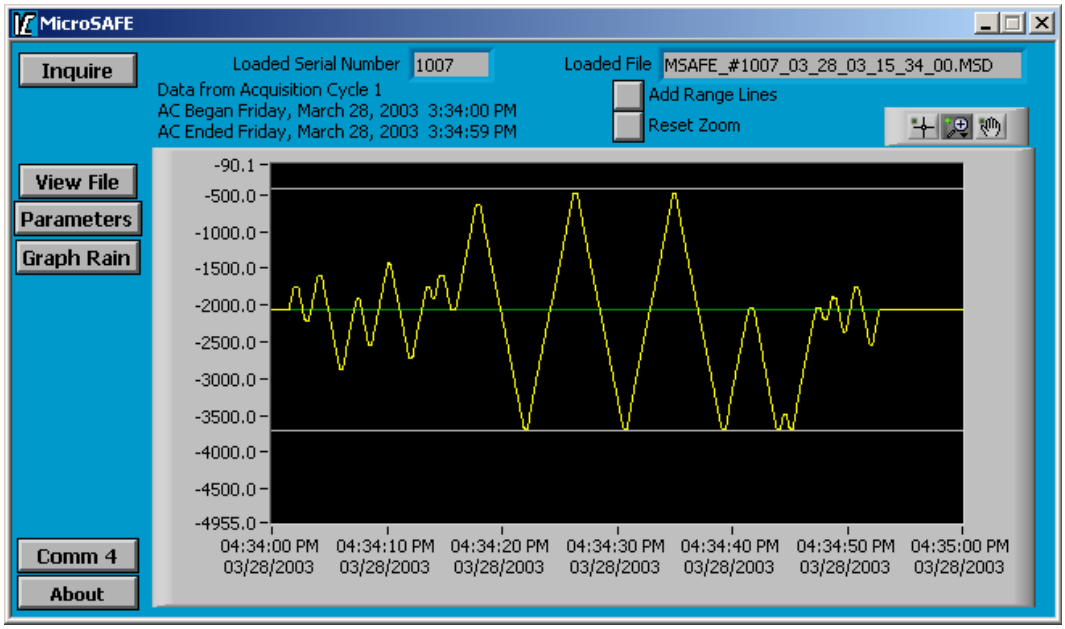

Figure 2.15: Strain History Induced During Milling Machine Tests

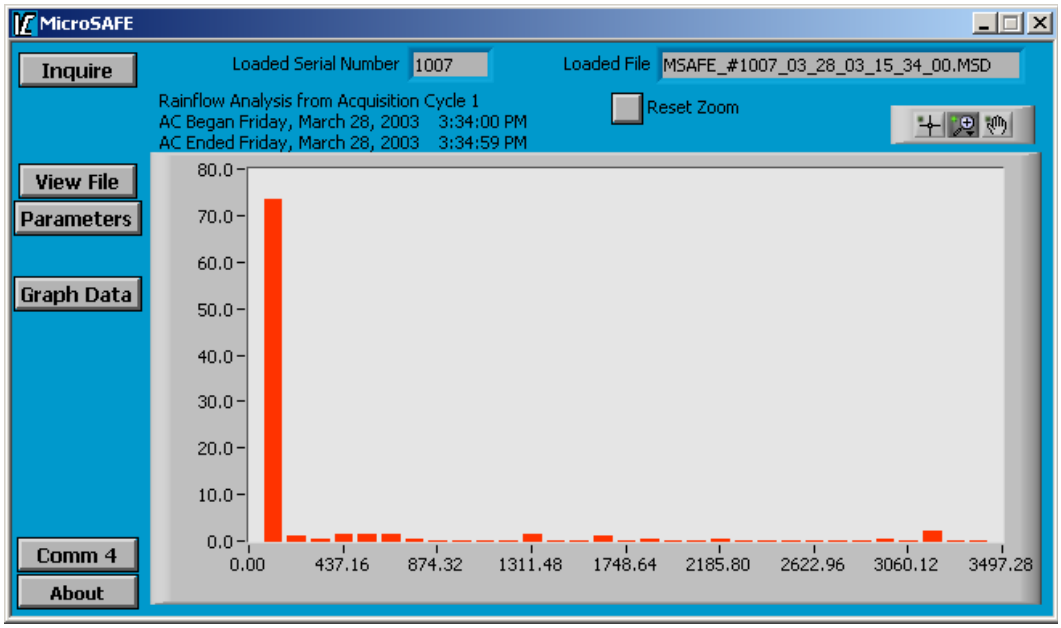

Figure 2.16: Rainflow Count from Milling Machine Tests

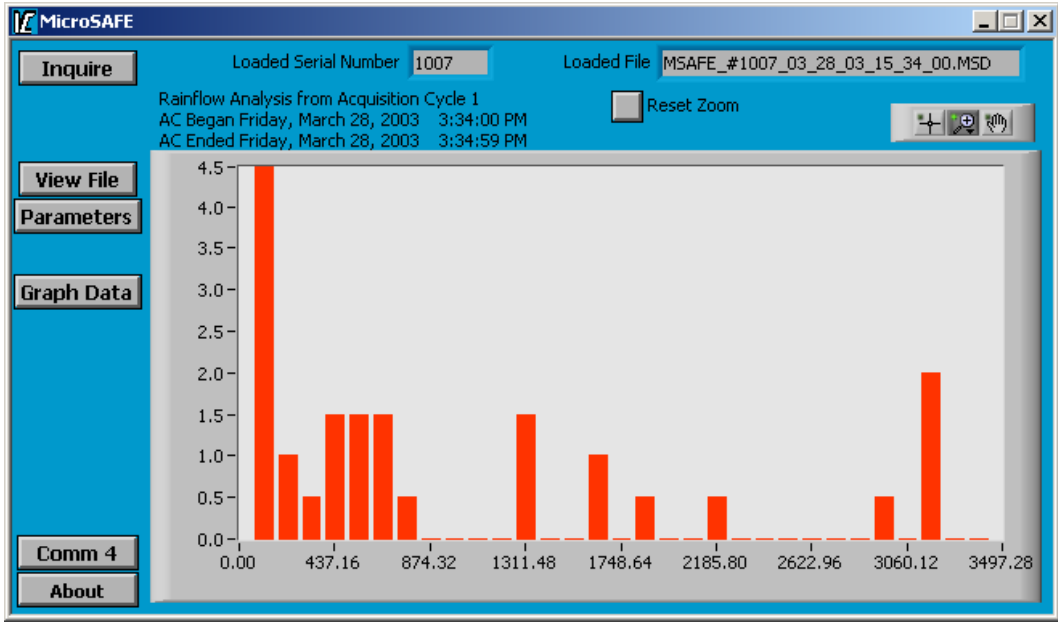

Figure 2.17: Rainflow Count from Milling Machine Tests with Background Noise Removed

2.3.5 Rainflow Verification

Following field-testing on the TX 71/US 183 overpass and testing on the CNC milling machine, many sets of raw strain data and corresponding rainflow data were available for analysis and confirmation. Two commercially available computer programs were used to verify the accuracy of the rainflow counting algorithm. The first of these programs, called "Crunch," is widely accepted in the structural analysis community (Buhl, 2003). The second program used for verification was a Matlab script available for download from MathWorks, Inc. This script allows the Matlab software package to

compute rainflow counts for any strain history, and is also widely accepted in the structural analysis field (Neislony, 2003).

Initially, ten 34-min strain histories were input into each program to verify that identical rainflow counts would be generated. Two of the examined strain histories are shown in Figure 2.19. Table 2.6 shows the resulting rainflow counts for these two strain histories. Both programs produced identical rainflow counts for each strain history examined.

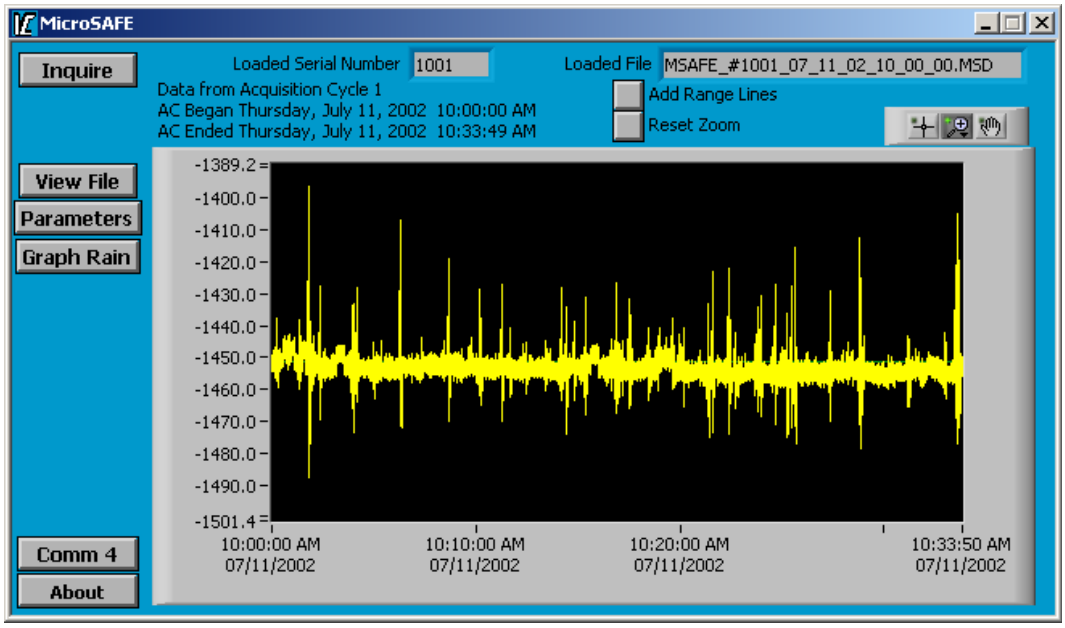

(a) Unit #1001

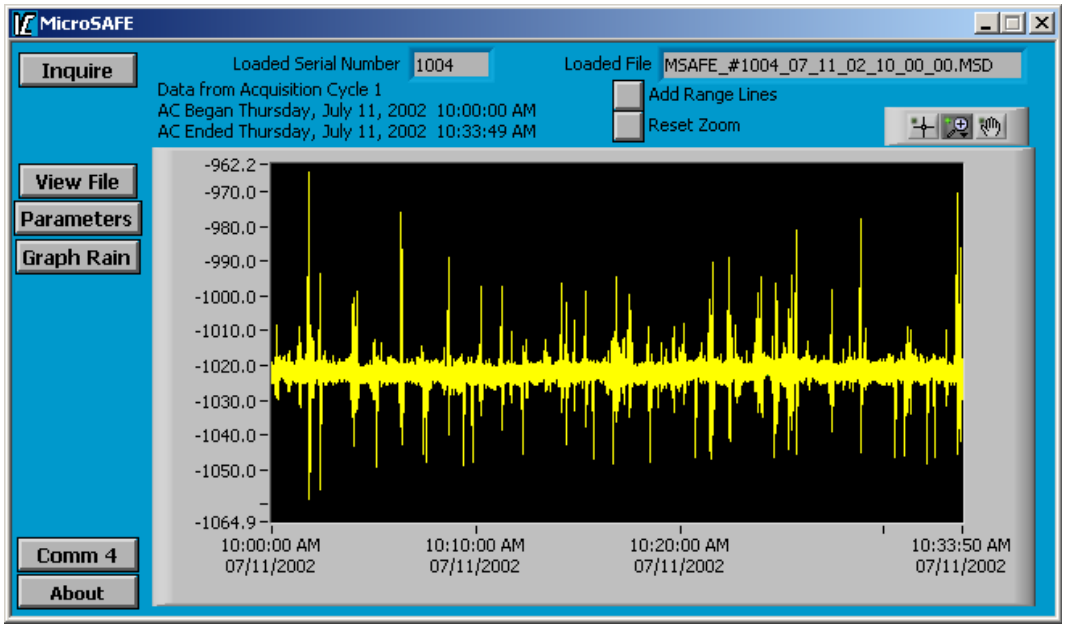

(b) Unit #1004

Figure 2.18: Strain Histories Used to Verify County Algorithms

Table 2.6: Verification of Rainflow Counting Algorithms

Bin (microstrain)	Number of Cycles			
	Unit #1001		Unit #1004	
	Crunch	Matlab	Crunch	Matlab
0-6	19707	19707	19856	19856
6-12	301	301	307	307
12-18	39	39	35	35
18-24	23	23	24	24
24-30	6	6	12	12
30-36	5	5	5	5
36-42	7	7	6	6
42-48	6	6	7	7
48-54	5	5	6	6
54-60	1	1	3	3
60-66	1	1	2	2
66-72	1	1	1	1
72-78	1	1	2	2
78-84	0	0	0	0
84-90	0	0	0	0
90-96	1	1	1	1
All other bins	0	0	0	0

Each program was also run using values taken from the example loading history depicted in Figure 2.1. This history was selected as a test history because the correct rainflow counts are know, given in the ASTM specification, and repeated again in Table 2.1. Both Crunch and Matlab produced the correct rainflow counts for this history. These results verified the accuracy of both programs, allowing either to be used as a benchmark for verifying the accuracy of the MicroSAFE algorithm.

When comparing MicroSAFE-generated rainflow counts to those generated by either Crunch or Matlab, results were not identical. Conversations with Invocon uncovered an error in the manner in the rainflow counting algorithm. Invocon has corrected the error and reprogrammed the units. Extensive tests were conducted to verify that the results agree with the cycle counts from crunch before the units were returned to the research team in October 2003.

The milling machine tests were repeated in December 2003 and all units are functioning properly. Plans have been made to initiate field tests on I-35 access ramps in Austin in early 2004.

CHAPTER 3:
INTRODUCTION TO SATELLITE NAVIGATION AND GPS

This chapter presents a brief history of satellite navigation systems and discusses a commercially available Global Positioning System (GPS) used for monitoring structural deformations. Global Positioning Systems are a relatively new method of locating points on and navigating the Earth. These systems use satellites in orbit high above the Earth that send radio signals to receivers on the surface. In their simplest description, modern GPS receivers gauge the distance from an individual satellite to a point. Four or more distance measurements are then used to determine a single position in four-dimensional space.

3.1 TRANSIT

The United States Navy developed the first satellite navigation system in the late 1950's for use in guiding nuclear powered submarines and launching Polaris intercontinental ballistic missiles. The missiles themselves were not guided by this system, but rather the launch point position was estimated for proper programming of the missile's on-board navigation systems. This first satellite navigation system, called *Transit*, comprised four to seven satellites in low-altitude, almost perfectly circular polar orbits.

With so few satellites, only one was in view at a given time. Precise clocks onboard each satellite relayed time data to receivers on the ships. *Transit* used the Doppler Effect, along with the transmitted time data, to determine the position of an object in the two-dimensional space of the earth's surface.

If the location (the orbit) of the moving satellite was known, the distance to a relatively fixed object (a ship or submarine on the ocean surface) could be computed. Velocity of the "fixed" object could be incorporated into the calculations to increase the accuracy of the location of an object. However, a 1 km/h error in the velocity estimate could create as much as a 200 m error in the reported position. Even with these errors, a nuclear warhead could still be launched at a target. However, because of these errors, other use of the *Transit* system was limited until more accurate positions could be obtained.

The passing of radio signals through the Earth's ionosphere and troposphere generated other problems. The Navy explored and adopted the use of dual-frequency transmitters (150 and 400 MHz) to aide in the removal of these errors. Modern GPS systems have retained this feature.

Two-dimensional positioning accuracy using the *Transit* system was approximately 25 m for a stationary object. Beginning in 1967, *Transit* was in limited use by other maritime organizations. If a stationary receiver collected continuous data for several days (hundreds of consecutive satellites passes), positioning data could be averaged to generate a three-dimensional position accurate to within 5 m. Better accuracy was realized when measuring relative distances from other fixed points. Accuracies of one meter were obtained over a distance of hundreds of kilometers when measuring satellite data concurrently at both points (Hoffman-Wellenhoff et al. 1997).

By the late 1960's, the benefits of satellite navigation were becoming clearer. Accurate three-dimensional positions could be measured anywhere on the globe without physical reference to a fixed point. All that was needed to increase accuracy was additional measurement time. As computing power and technology advanced, satellite navigation systems became even more accurate (Mirsa and Enge 2001).

3.2 GPS

What eventually became the Global Positioning System (GPS) is use today began in the early 1970's with a joint venture of the United States Navy and Air Force, under the direction of the Department of Defense. Technology had advanced far enough to create a more accurate system than *Transit*. This new system would generate a more accurate three-dimensional position in far less time.

By the late 1970's, clock technology had improved to the point where the internal clocks on each satellite could be perfectly synchronized. A more accurate position could be computed with increased speed, providing that more satellites were in view of a single receiver and that each satellite could output its position and time more accurately than before. A medium Earth orbit of 5,000 – 20,000 km was chosen to allow a relatively small constellation of 24 satellites to blanket the Earth with coverage. With this system, any single receiver would have between four and twelve satellites in view at any given time. Each satellite had the potential to stay in view of a stationary receiver for a few hours, allowing significantly longer data acquisition than the 10 - 20 min viewing times for *Transit* satellites.

Choosing the orbital distance for the satellites required some compromise for designers. Satellites with increased orbital distance from Earth are more expensive to launch and require more signal power to transmit their signals back to Earth. However, as orbital distance is reduced, each satellite would have a shorter viewing window for a given receiver, requiring more satellites. For these reasons, the medium Earth orbit and constellation of 24 satellites was chosen.

The choice of a transmitter frequency band took into account a number of factors. Higher frequencies lessen ionospheric and tropospheric frequency refraction, but increase signal strength loss. The L-band of frequencies (1-2 GHz, fairly low in the spectrum and relatively uncluttered at the time) was chosen to combat these effects.

Designers also faced the decision of whether GPS would be a passive or an active system. Passive satellites transmit data to ground receivers but do not receive any data in return. Active satellites would have two-way data transmission capabilities. The main military advantage of the passive system is that it allows anonymity of position for the GPS user. Military personnel could generate accurate positions without giving away their own. In addition, it would allow an unlimited number of receivers to operate at a single time. The choice of a passive system was obvious.

A minimum of three satellites must be in view at all times for dual-frequency GPS to produce the most accurate three-dimensional position. Clocks onboard each satellite must maintain perfect synchronization with each other to produce the best ranging calculations. Clocks within the GPS receiver must also remain perfectly synchronized with the satellite clocks. This presented a dilemma that would be very expensive to solve. The simplest solution, however, was to employ inexpensive quartz clocks in each GPS receiver. These clocks would keep accurate time, but would not be synchronized with those onboard the satellites. The timing error between the receiver clock and each synchronized satellite time would be identical (called *receiver clock bias*). The use of data from a fourth satellite would remove this time bias and allow for the most accurate of measurements in four-dimensional space (three space dimensions, one time dimension) without the expense of synchronizing receiver clocks.

A final caveat to GPS measurement is that vertical positioning values are less accurate than horizontal positioning values for any GPS receiver. This phenomenon can be explained by understanding the geometric relationship between a single ground-based GPS receiver and the constellation of orbiting satellites. The majority of satellites in view of a ground-based GPS receiver will be closer to the horizontal plane tangent to the Earth at the point of GPS reception than to the vertical axis running directly through the GPS receiver. There may be a few satellites located "above" the GPS receiver, but not nearly as many as "to the sides" of the receiver. A GPS station moving horizontally will move farther from the satellites "to the side" of it than those "above" it. The opposite is true for GPS stations moving vertically. These stations will move farther from the satellites above the station than those to the sides. Larger changes in distance will generate more accurate results, since the distance changes will be greater than the background noise level. For these reasons, horizontal movements will be easier to resolve than vertical movements.

With all apparent problems solved, system architecture was approved by the Department of Defense in 1973. The first satellite was launched in 1978, but the system was not deemed operational until 1995. Over $10 billion was invested in the system, and $500 million per year is spent for its upkeep (Mirsa and Enge 2001).

The military's goals with GPS were to obtain velocity, distance, and time measurements quickly and accurately for use against its enemies in a variety of ways. Like any weapon, it would be most useful if the enemy were not allowed access to it. Upon verification of the accuracy and usability of the system, plans were devised to allow only the government access to the most accurate GPS positioning data.

In the early 1990's, GPS signals were encrypted and could only be decoded by those with the appropriate key – the federal government. By the mid 1990's, civilian objection to signal encryption had grown strong enough to cause a change in GPS signaling. A new plan was instituted, called Selective Availability, where non-encrypted signals were distributed, free for use by anyone. Errors were pre-programmed into these signals, changing horizontal positioning accuracy from approximately 10 m to 500 m. Only the military would have prior knowledge of these randomly generated errors and be able to remove them to obtain the best accuracy. Selective availability allowed civilian use of GPS, but not with enough accuracy to do any significant military damage (National Academy of Sciences, 1995).

Unfortunately for the United States government, other nations began to experience acceptable accuracies using their own GPS satellites and hardware. The need for selective availability was rapidly diminishing. On May 2, 2000, a Presidential Order decommissioned Selective Availability. The most accurate GPS signals were now available to everyone.

3.3 PRESENT DAY GPS

Since the Presidential Order canceling Selective Availability, very accurate global positioning data have been available to the entire world. Civilians can now spend about $100 and purchase a pocket-sized GPS receiver that can calculate a variety of variables with the push of a button. Horizontal positioning accuracy on these units is as low as 5 m. Vertical positioning accuracy, as with any GPS receiver, may be double this value or more. These personal GPS receivers can calculate distance traveled, velocity, bearing, heading, elevation, latitude, longitude, time-zone changes, and even draw a scalable map as you travel. As long as a clear view of the sky is maintained, positioning errors remain small, even for these very basic and inexpensive systems.

Upon the removal of Selective Availability, the commercial market for GPS boomed. Many companies now offer survey-grade equipment that can be purchased for $10,000-50,000 per receiver. This level of equipment can generate accuracies of approximately 10 mm in a relatively short amount of time. Automobile manufacturers have begun to adapt GPS receivers into their cars as navigation aides. Personal watercraft manufacturers have followed to aid in open-water navigation. These interactive systems can integrate destination information and position information to guide the user with great accuracy and speed.

3.3.1 Differential GPS

For the majority of users, positioning values within a few meters of the actual location are sufficient for navigation. However, for surveying the location of a structural component, more accurate measurements are required. Differential dual-frequency GPS equipment is often employed to obtain the best possible GPS measurements.

Differential GPS employs two or more GPS receivers working together, communicating with each other via radio. One receiver is fixed over a known position, while the other "rover" unit is stationed on the object to be monitored. The rover unit takes positioning data relative to the known location of the fixed unit. The fixed unit must be within proximity (a few kilometers) of the rover at all times, so that the same satellite signals are being received and processed by both units. Since the location of the fixed point is known and each unit is processing the same satellite signals, most errors caused by atmospheric effects can be considered and neglected. This method of GPS measurement can result in very accurate positioning values, usually within 10 mm of the actual position in the horizontal plane.

3.3.2 Striving for Better Accuracy

Two types of errors exist when acquiring data in any situation: random errors and systematic errors. One possible systematic error in GPS is frequency shift. As the satellite signal passes through different atmospheric layers, its frequency can change, changing the apparent position of the receiver. Each signal passing through a given layer at the same time will encounter the same frequency shift. However, random errors may result from the constantly changing thickness of these layers, from random satellite transmission interruption, or a variety of other causes. Using more than one GPS receiver for a given position calculation allows the removal of systematic errors. One receiver acts as the control to the GPS experiment, while the other receiver(s) act as variables. This scientific method of problem solving greatly aids in improving positioning accuracy due to the removal of systematic errors.

Unfortunately, a GPS user must still consider random errors. Random errors cannot be completely removed, but averaging can diminish their experimental effects. When data are collected at a fixed point and averaged, effects from randomly occurring errors can be dramatically reduced. As more data are averaged over a longer period, the likelihood of encountering the both positive and negative random errors increases. As more errors of varying signs are encountered, they begin to balance out, improving positioning accuracy. The data presented in Chapter 4 will show that experimental accuracy generally improves with averaging time, but does have some exceptions.

Dual-frequency differential global positioning systems provide the most accurate satellite positioning information currently available. When data from these units are averaged over time, positioning should become increasingly more accurate.

3.4 NETFORCE GLOBAL POSITIONING SYSTEM

This section will review the testing and evaluation of a commercially available, dual-frequency, differential global positioning system. Mezure, Inc., located in Bend, Oregon, developed this system, called NetForce. NetForce was developed to measure very small displacements of an object over a long period of time (weeks, months, years, etc). This report will examine the NetForce system as it would be used to observe long-term structural deformations of various bridge components. Examples of these components may include, but are not limited to, vertical or lateral deflections of suspension bridge towers due to temperature changes or settling of cable anchor blocks over many months or years.

The NetForce system will be evaluated for its accuracy and applicability to monitoring various parts of major and unique TxDOT bridges. Mezure has advertised “sub-centimeter” level accuracy for the NetForce system. The system will be fully evaluated for its accuracy and the time required to achieve this accuracy.

To be fully applicable to TxDOT in the area of bridge monitoring, centimeter-level or better accuracy will be required. As testing results are presented, the applicability of the system will be discussed further.

3.4.1 NetForce System Operations

NetForce is a “plug and play” wireless system, where the system can be ready to take GPS data only moments after the equipment is delivered and power provided. Stand-alone weatherproof enclosures containing all hardware necessary for GPS measurements are delivered to the site and attached to the object that requires monitoring. Raw, unprocessed GPS data are received by the antenna, located within the fiberglass enclosure (which is relatively transparent to GPS signals), and logged by the receiver. An internal cellular modem encrypts the data, transforms them into packet form, and transmits them via a digital cellular signal. This service acts as a normal cellular telephone connection, except that the connection is always active, enhancing signal reliability.

After the cellular provider receives the data, as shown in Figure 3.1, they are then transmitted over a broadband Internet connection to Mezure’s Network Operations Center (NOC), located in Bend, Oregon.

Data are also sent to a series of remote mirror sites where copies of all data are stored. This allows the retrieval of past GPS data if there is a problem within the system.

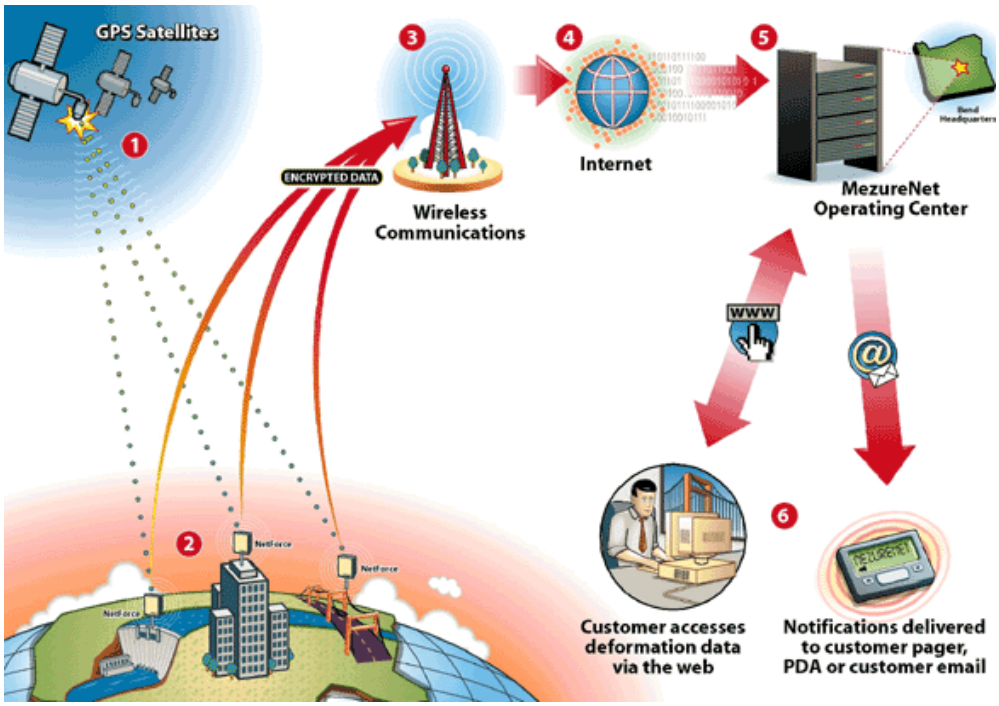

Figure 3.1: NetForce System Operations

Processing of the raw GPS data, called post-processing, is done by Mezure at the NOC. Unprocessed GPS data are stored in RINEX format (Receiver INdependent EXchange), which is widely accepted in the GPS field. RINEX data are processed using software by Novatel to obtain the actual coordinates of each GPS station in three dimensions. The horizontal coordinate values are given in degrees of Latitude and Longitude. The vertical coordinate is given in meters above mean sea level (MSL). A conversion formula was used to transform the horizontal coordinate values from units of degrees into units of meters. Once all three dimensions are referenced in units of meters, displacements can be computed by subtracting the coordinates of successive positions.

3.4.2 MezureNet Website

Users can access their GPS data at any time through a password-protected website called MezureNet. Each customer will have a custom website designed specifically for their set of NetForce stations. Customers can have a single or multiple passwords that allow them to view the current state of each GPS station through the Internet.

When a customer logs on to their MezureNet website, they are presented with an overview of the positions of each NetForce station. Each station is presented with a customer-specified name (“North Tower 1” or “West Abutment,” for example). A photograph of each station can also be incorporated for easy station identification and user friendliness, as shown in Figure 3.2.

Figure 3.2: MezureNet Home Screen

Eight color-coded horizontal bar charts present the current state of certain parameters associated with each station, as seen in Figure 3.2. A consistent blue bar chart with a centered green square indicates that the value of that parameter is centered within its specified limits. If the green square moves off center, that parameter is approaching a limit value. When the entire bar chart is colored red, that parameter has exceeded its specified limits. An event that exceeds limits will trigger an alarm, which would in turn alert the user of a potential problem.

When navigating the website, the user can place the mouse pointer over each bar chart. This will display the last reported value of the associated parameter and the specified limit value. Each parameter's characteristics and definitions are given below:

- *Data Gap* – The amount of time, in seconds, since the station last reported GPS data to Mezure's NOC. The limit specified by Mezure is 300 s, but rarely does the actual value vary from 0 s. Units are very good at reporting data promptly and on time.
- *Horizontal Uncertainty* – The +/- margin of error, expressed in meters, of the horizontal position calculations with a confidence level of approximately 68% (1 standard deviation in two dimensions). The limit specified by Mezure is normally 0.1 meters. Observed values usually hover around 0.01-0.03 m.
- *Vertical Uncertainty* – The +/- margin of error, expressed in meters, of the vertical position calculations with a confidence level of approximately 68% (1 standard deviation in two dimensions). The limit specified by Mezure is normally 0.1 m. Observed values usually hover around 0.01-0.03 m.
- *Position Type* – This signifies the strength of the position solution obtained by the GPS software. As satellites move in and out of range, or on-site conditions change, communications lock with each satellite may be compromised, causing a decrease in position type. Position Type ranges from zero (the best GPS solution) to 10 (the worst GPS solution). Limit values are normally set at 3.5, but rarely deviate from zero.

- *Down / Up* – Displacement along the vertical axis, in meters, from the control coordinate (a starting location for each GPS station that can be reset at any time). Limit values are user-set.
- *East / West* – Displacement along the east/west horizontal axis, in meters, from the control coordinate. Limit values are user-set.
- *North / South* – Displacement along the north/south horizontal axis, in meters, from the control coordinate. Limit values are user-set.
- *Horizontal Radial* – Straight-line displacement, in meters, from the control coordinate along the horizontal plane. This is derived using the Pythagorean theorem of right triangles and the values of East/West and North/South. Limit values are user-set.

The reference station will have its own information panel on the MezureNet website, similar to those for each rover station. However, only values for the Data Gap parameter will be displayed for the reference station. Since the reference station is stationary, displacement values are calculated relative to its position. Therefore, the reference station needs only to output its position reliably to maintain accuracy over the entire system. A stationary reference point makes differential GPS possible.

3.4.3 Graphical User Interface

MezureNet users can view plots of displacement versus time for each NetForce station. The "View Graphs" button on the information panel for each station will open a new Internet browser window. Three plots of displacement versus time are visible in this view port: latitude, longitude, and vertical. All three dimensions of displacements are plotted in meters.

Users may select to plot measured displacements over various amounts of time. These times include 1, 3, and 12 hr, 1, 3, 7, and 14 days, 1, 3, and 6 months, and 1, 2, 3, 4, 5, and 10 yr. By selecting the desired timeframe, each plot will be automatically rescaled using the most current positioning information.

One-hour plots allow the user to see individual 10-sec data points, along with the 5-min average points computed during that hour. These first averaging points begin show improved accuracy and clustering when plotting the displacement of a fixed position, as shown in Figure 3.3.

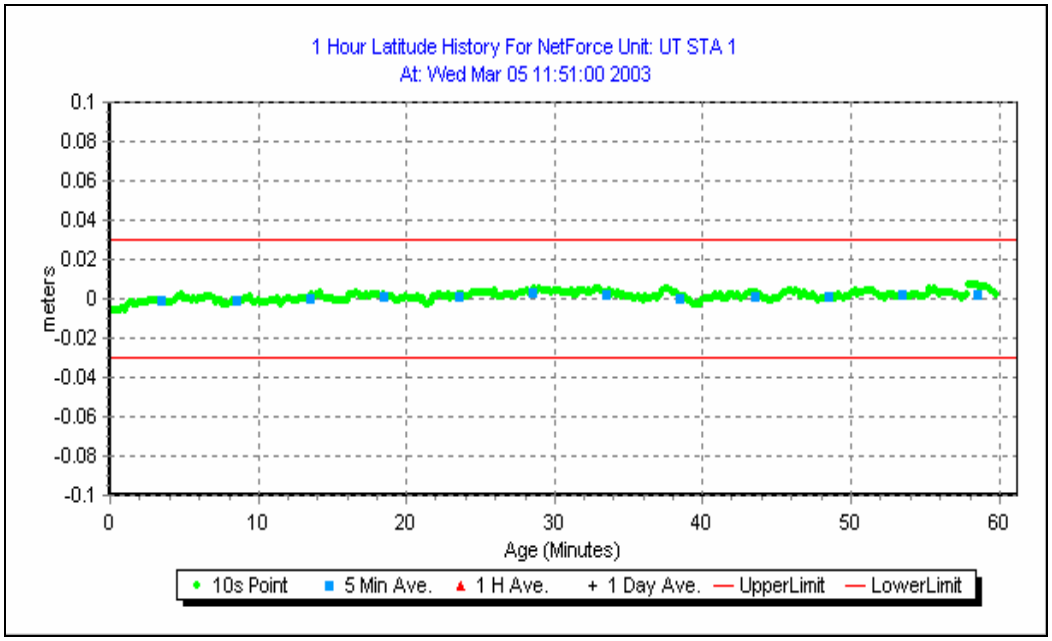

Figure 3.3: One-Hour Latitude Displacement Plot

Three-hour plots show 10-sec data points, 5-min average points, and begin to show 1-hr average points. As the length of time plotted is increased, more frequent data points become obscured by the average points. When only averaged positions are plotted, a trend line of average displacement behavior is established. This trend line is a more accurate representation of the displacement behavior of that station over the long term (see Figure 3.4).

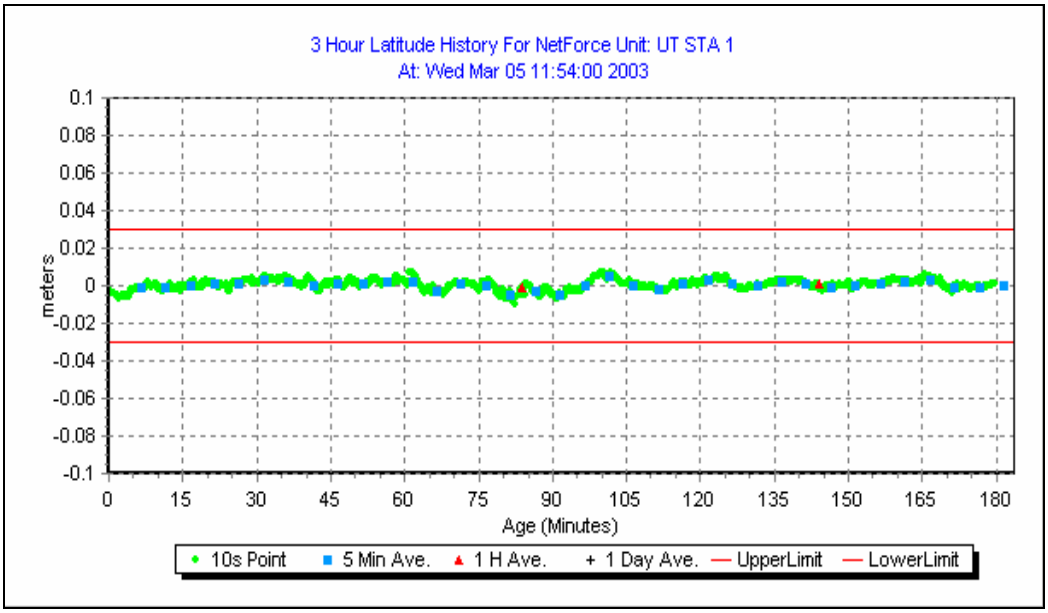

Figure 3.4: Three-Hour Latitude Displacement Plot

Horizontal red lines represent user-specified limit values for displacements in each dimension. When measured data exceed these limits for a user-specified amount of time, an alarm can be triggered to alert the customer of the situation.

3.4.4 Data Download

Blocks of data acquired by the NetForce system are available to the user over the Internet. Unprocessed RINEX data can be downloaded in 24-hr segments through the Mezure website. The previous five days of raw data are stored for each NetForce station. RINEX data sets older than five days are available, as well, but only upon special request.

3.4.5 Displacement Limits and Alarms

The majority of NetForce users will elect not to perform their own post-processing of the raw GPS data. NetForce facilitates the outsourcing of data processing and interpretation duties, so that the end user can be free to perform other tasks. When the displacement of a monitored structural component exceeds rational limits, that is the time when the customer would like to be alerted. This directly defines what the Mezure system does best. Mezure's software and hardware monitors the stations without any personal attention, 24 hours a day. When displacements have exceeded customer-specified limits, the customer can be alerted to it in a variety of ways. These may include a personal telephone call or automated messages delivered via e-mail, pager, or personal data assistant.

3.4.6 Special Considerations

Units can be programmed to report a position as often as every 10 seconds, or as infrequently as the user wishes. However, as the reporting speed is increased, monitoring costs also increase.

On sites where cellular service is not yet available, a special cellular hub can be set up on-site for the exclusive use of the GPS modems. This hub will receive data from each NetForce station and transmit them via a dedicated Internet connection to Mezure's NOC. Once again, system costs will escalate with this requirement.

Alternating current (120 VAC) normally powers the NetForce units. Inside the weatherproof enclosure, a step-down transformer converts 120 VAC to 12 volts of direct current (VDC). The direct current supplies the power needs of both the GPS receiver and cellular modem, as well supplying the internal backup battery with current.

On sites where 120 VAC service is not accessible, each NetForce unit can be connected to a solar panel for remote powering. These panels power the hardware and recharge the internal backup battery during the exposure to sunlight. The backup battery powers the hardware during dark hours. Mezure has employed high-power cellular modems that draw very little current from the power supply. The GPS receiver itself also uses very little current, allowing reliable use of the solar panel. In the event of an external power loss, a fully charged backup battery will last approximately 30 hours during continuous operation.

Finally, when a project requires multiple GPS antennas to be in close proximity to each other, each GPS antenna can be mounted in any location with a clear view of the sky, while the GPS hardware package can be mounted away from this location. This will permit the cellular modems to transmit clearly without creating interference. Should GPS need to be employed in aesthetically sensitive areas, this technique can also be used to disguise the bulk of the GPS hardware by hiding it away from view. Accuracy of the data is not influenced by the distance between then antenna and the GPS hardware.

CHAPTER 4:
EVALUATION OF COMMERCIAL GPS DATA

This chapter discusses the collection and evaluation of data from the commercial global positioning system (GPS), NetForce, by Mezure, Inc. The conceptual design of the evaluation procedure and detailed design of the experiments used to evaluate the sensitivity of the results in the horizontal and vertical planes will be discussed. Important GPS data will also be presented.

4.1 CONCEPTUAL DESIGN OF EXPERIMENT

The focus of this experiment was to determine if the GPS data were sufficiently accurate to be used by TxDOT for the long-term structural health monitoring of bridges. On TxDOT's major and unique bridges, the Engineer or Inspector might wish to monitor the movement of components of the bridge at certain points over the long term. These may include the top of a support tower, mid-span of a bridge deck, suspension cable anchor blocks, or stay cable anchorage points. It would be important to monitor the location of each these points in three-dimensions with a certain degree of accuracy. This degree of accuracy must allow the user to measure movements that may signal the onset of a structural problem. On some structural components, a single centimeter (or less) of displacement could create a structural problem, while on other components, daily thermal fluctuations of a few centimeters may be common and overlooked. The user may wish to measure deflections relative to stable ground or relative to another point on the structure. To fulfill these requirements, a global positioning system would therefore need to be versatile in its installation capabilities and highly accurate in its three-dimensional measurement capabilities.

4.1.1 Overview of Test

Mezure loaned three GPS stations to the project team for testing purposes. One station remained stationary at all times and served as the reference point for the remaining two stations. The remaining two stations, called rovers, were placed away from the reference point. These stations were moved in a controlled manner to generate displacement data relative to the fixed reference station. Two rover stations were used to determine the repeatability of the experimental data. For the majority of bridge monitoring situations, the reference station would not be placed on the bridge. Relative displacements would therefore be measured from a known, fixed point.

To create the experiment, the rovers were displaced by known amounts to simulate the variety of scenarios that may be encountered on an actual bridge. Displacement data were then collected from these two stations, compared with the known displacements, and analyzed to determine the accuracy and sensitivity of the measurements. In each of the displacement sequences discussed in the following sections, nominally identical displacements histories were imposed on both rover stations.

Figure 4.1 shows the general layout of the testing site. The area pictured is the southwest corner of the J. J. Pickle Research Campus at the University of Texas at Austin. Both rover stations were placed near the center of a large field that would provide a clear view of the sky and the best possible GPS signals. It was desired to test the capabilities of the system for a long-span bridge installation, where a rover may be located relatively far from its reference station. Accuracy of the GPS solution for a particular rover station will decrease as the distance between the rover and the assigned reference station increases. Therefore, the reference station was placed 560 ft from the rover stations.

The rovers were placed as close to each other as possible to remove experimental differences caused by environmental variables such as atmospheric signal disturbances. Because of the high-power cellular signals being transmitted by each rover station, it was recommended by Mezure that the stations be separated by at least 100 ft. Therefore, the rovers were placed approximately 100 ft from each other, as shown in Figure 4.2. Each rover station was attached to a 20" x 20" x 28" concrete block. Each block weighed approximately 1000 lb.

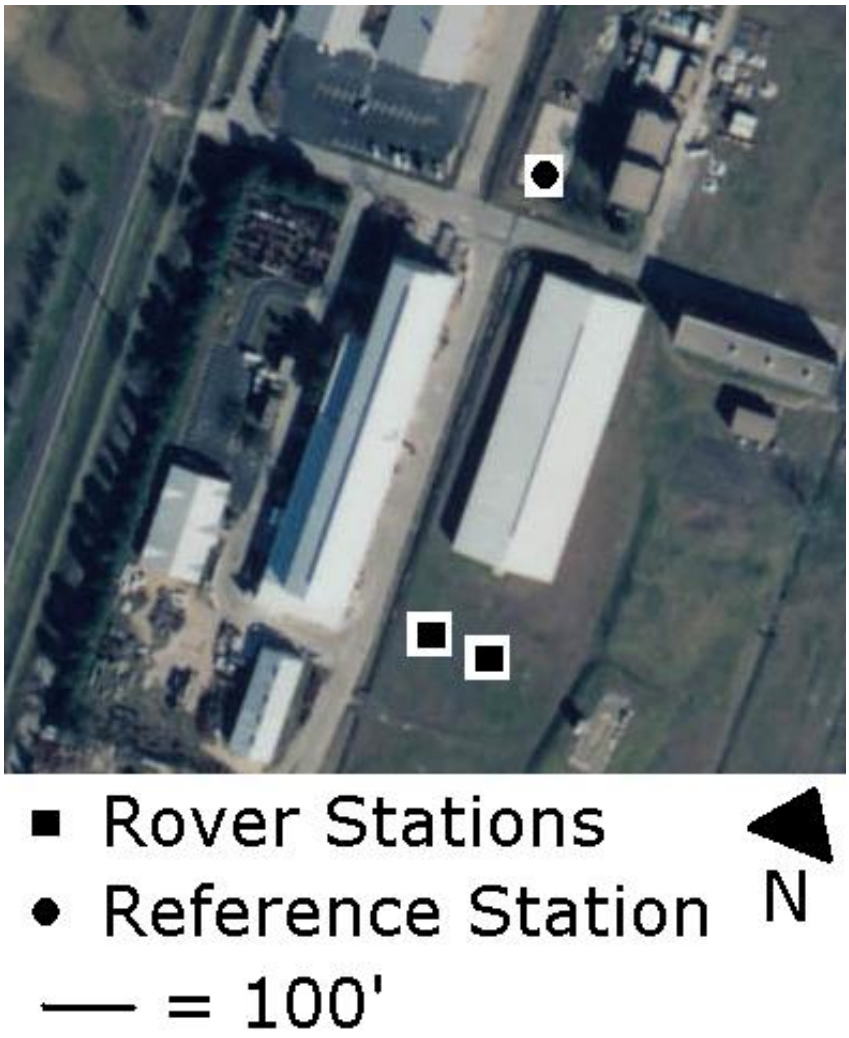

Figure 4.1: Testing Site Layout

The reference station used in this experiment is shown in Figure 4.3. The hardware package for the reference station is exactly the same as for the rover stations, and will be described further in Section 4.1.2. To assure a fixed position, the NetForce hardware package was bolted to a 24" x 24" x 30" reinforced concrete block. Power was provided from a nearby building.

The elevations of all three stations are approximately the same. The large buildings shown in Figure 4.1 to the north and west of the rover stations are not more than 40 ft in height. Short structure heights combined with distance from the structures help to reduce multipath effects to acceptable limits. Multipath effects, depicted in Figure 4.4, are caused by satellite signals being reflected off the ground, surrounding structures, or anything else that does not absorb radio waves. When the signal is reflected, it travels farther than a direct satellite signal. This extra distance requires additional travel time, giving the illusion that the satellite is farther away than it actually is. Normally, shielding on the underside of the GPS antenna absorbs some of the ground reflection. Unfortunately, it is not possible to shield against all reflective paths. These signals must be minimized to obtain the best GPS signals. For these reasons, all stations have a clear view of the majority of the sky at all times. This is the most important key to any successful GPS station installation.

Figure 4.2: Layout of Rover Stations

Figure 4.3: Layout of Reference Station

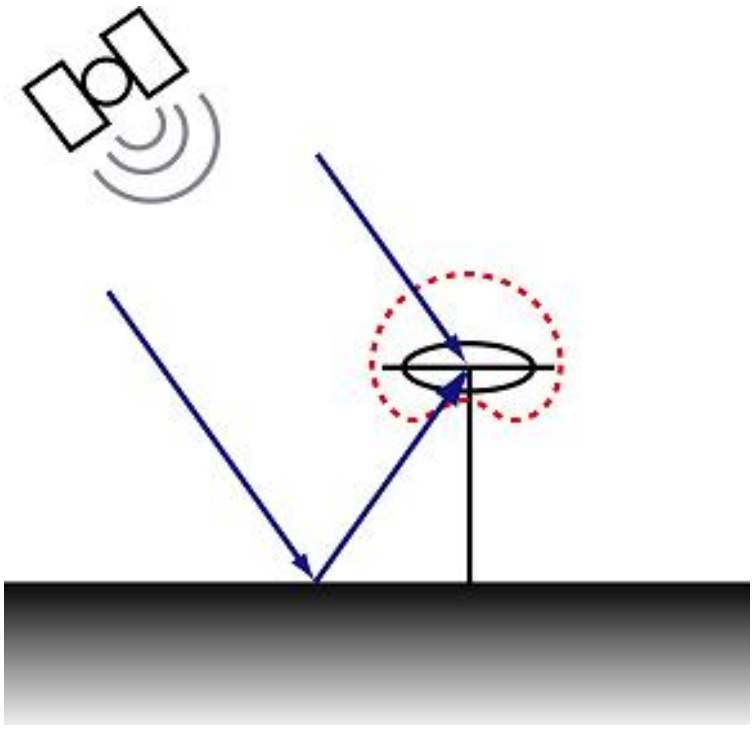

Figure 4.4: Ground Reflection Multipath Signal (Bilich, 2002)

The nature of the global positioning system dictates that the measured data in the vertical plane will be less accurate than the measured data in the horizontal plane, as mentioned in Chapter 3. On single-receiver systems, the decrease in vertical positioning accuracy ranges from 40% at a 95% confidence level to 67% at a 99.99% confidence level over the measured horizontal position accuracy. Therefore, if the horizontal component of the actual position were measured to be within 1.0 m of its true position with a 99.99% confidence level, the vertical component of the actual position could only be measured within 1.67 m of its true position at the same confidence level (Hofmann-Wellenhof, et al., 1997).

Because of the difference in horizontal and vertical positioning accuracies, testing in the horizontal and vertical planes was divided into two separate phases. Testing of the GPS in the horizontal plane was conducted first, and will be discussed in Sections 4.2 and 4.5. The second phase involved vertical axis testing of the GPS, and will be discussed in Sections 4.3 and 4.6.

4.1.2 Hardware

Each GPS station is enclosed within a 10" x 16" x 18" weatherproof fiberglass enclosure, shown in Figure 4.5. This enclosure and associated hardware weighs approximately 50 lb and was delivered fully assembled as shown in Figure 4.6. All necessary hardware for the operation of the each GPS station is located within this enclosure.

Hardware within each GPS station can be divided into five components: the GPS antenna (white disk located at the top of Figure 4.6), the GPS receiver (black box located immediately below the GPS antenna, situated horizontally), the cellular modem (black box located immediately below the GPS receiver, situated horizontally), the power supply (black box toward the lower-left corner of the enclosure), and the backup battery (black box toward the lower-right corner of the enclosure). The GPS antenna is responsible for receiving the radio signals transmitted from the orbiting satellites. The fiberglass enclosure does not interfere with communication between the satellites and the GPS antenna.

After the antenna receives the satellite signals, the GPS receiver sends them via serial cable to the cellular modem. The modem then transmits the signals to Mezure's Network Operations Center (NOC) via cellular signal and the Internet.

Figure 4.5: GPS Hardware Package

Mezure has designed the complete hardware package to be mounted to the structural component(s) that will be monitored. When the structural component displaces, the hardware package will displace with that component. This will displace the antenna and the GPS data will be used to monitor the structural component.

Mounting the GPS unit is facilitated through the use of the supplied mounting bracket. This bracket is a galvanized steel cradle, shown around the base of the fiberglass enclosure in Figure 4.5, which can be bolted to any object using appropriate anchors. Once the bracket is mounted to the structure, the GPS enclosure is seated in the cradle and bolted from within. When mounting is complete and 120 V AC power is supplied to the unit, the GPS hardware can be switched on and data collection can begin immediately.

Figure 4.6: GPS Hardware Package (cover removed)

4.2 HORIZONTAL TESTING SETUP

In order to evaluate the accuracy, sensitivity, and repeatability of the horizontal GPS data, a mechanism was developed to move the rover stations in a controlled manner. The entire station would have to be stable against wind and rain forces, and it must have the flexibility to allow horizontal movements in any direction.

To facilitate these requirements, large concrete blocks were selected as the foundations. Each block was leveled after positioning in the open field (Figure 4.2). A Palmgren two-axis milling table (Figure 4.7) was bolted to the top of each concrete block. Milling table dimensions and directional precision data are presented in Table 4.1.

Table 4.1: Milling Table Specifications

Quantity		Dimension
Table Length	A	18-5/8”
Table Width	B	6”
Table Height	H	5-3/16”
Base Length	L	12”
Base Width	W	7-1/8”
East-West Travel		12”
North-South Travel		8”
Travel per revolution of adjustment screw		0.0787”
Reported precision of displacements		0.0008”
Actual precision of displacements		0.009”
Weight		60 lb

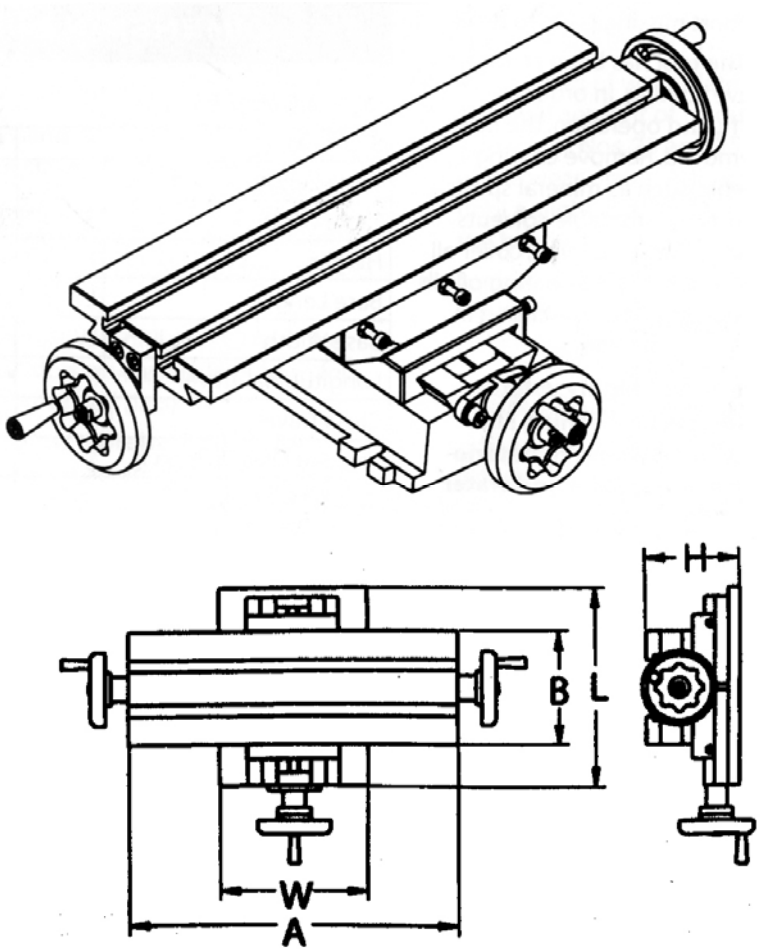

Figure 4.7: Palmgren Milling Table

The precision of each adjusting screw was specified by Palmgren to be 0.0008". However, because of backlash present in the adjusting screws, a reduced level of precision would be realized when changing direction. Assuming that a reversal of direction might occur during any test, both east/west and north/south precision were taken as the backlash present in the adjusting screws, 0.009". This level of precision for horizontal movements was taken to be sufficient given the reported level of accuracy of the NetForce system.

The GPS hardware package was attached to the milling table. The completed apparatus, (Figure 4.8), allows the precise movement of the GPS hardware enclosure in two directions within the horizontal plane.

Figure 4.8: Horizontal Testing Apparatus

4.3 VERTICAL TESTS

In order to evaluate the accuracy, sensitivity, and repeatability of the vertical GPS data, a mechanism was developed to move the rover stations in a controlled manner. As with the horizontal movement package, the entire station would have to be stable against wind and rain forces, and it must have the flexibility to allow vertical movements.

Upon completion of the horizontal testing phase (Section 4.5), the horizontal testing apparatus was altered to allow vertical movements. This was done by unbolting the GPS hardware enclosure from the milling table base, inserting rectangular steel shims of varying thickness, and attaching the enclosure to the

milling table using C-clamps. The C-clamps allowed quick and easy insertion (or removal) of shims that would displace the station in the vertical plane by known amounts.

To induce a vertical displacement, shims were added or subtracted from beneath the GPS enclosure. After a vertical displacement was induced (positive or negative) and the station reaffixed to the milling table, the shim stack would be measured at all four corners. Measurement was performed using a dial caliper with an accuracy of 0.001". These four values were averaged and this number taken to be the mean height of the station above the milling table surface. The actual value of the induced vertical displacement was then calculated by subtracting the new station height from the previous station height.

4.4 PROCEDURE USED TO EVALUATE GPS DATA

The procedure used to evaluate all the GPS positioning data is described in this section. Although GPS stations were fixed for some experiments and subjected to a variety of different displacement histories in other experiments, the same evaluation method was used in all cases. Note that the GPS data used in all analyses are raw GPS position data sent directly to the research team from Mezure. One position value is reported by the GPS stations every 10 sec. These are not the data that can be seen in the GPS position plots found on the MezureNet website; however, using the raw data provided the research team the opportunity to evaluate the data more thoroughly.

A simple displacement history is shown in Figure 4.9. At time t_o, the GPS unit is moved from position x_A to x_B. The actual distance moved, $\Delta x = x_B - x_A$, is measured on the milling table by multiplying the number of crank revolutions by the travel per revolution listed in Table 4.1.

The GPS data recorded for the interval are plotted in Figure 4.10. Before t_o, the average value of the measured GPS data is $\bar{y}_A$ and after t_o, the average value of the measured GPS data is $\bar{y}_B$. Under ideal conditions, the difference between the two average positions, $\Delta GPS = \bar{y}_B - \bar{y}_A$, should equal the actual distance moved, Δx. However, the GPS data contain errors for the reasons described in Section 3.2. Therefore, ΔGPS will be compared with Δx to evaluate the accuracy and sensitivity of the GPS data.

One consequence of the setup used is that the rover GPS units were not repositioned instantly. Therefore, when comparing the GPS data with the actual displacement histories, it is important not to consider the period of time when rover GPS units are being moved. As shown in Figure 4.11, this period is called the block-out period, and is centered about the reference time t_o. To be conservative, the entire block-out period was assumed to be 10 min, centered about t_o. Individual block-out times (t_b) were five minutes in duration.

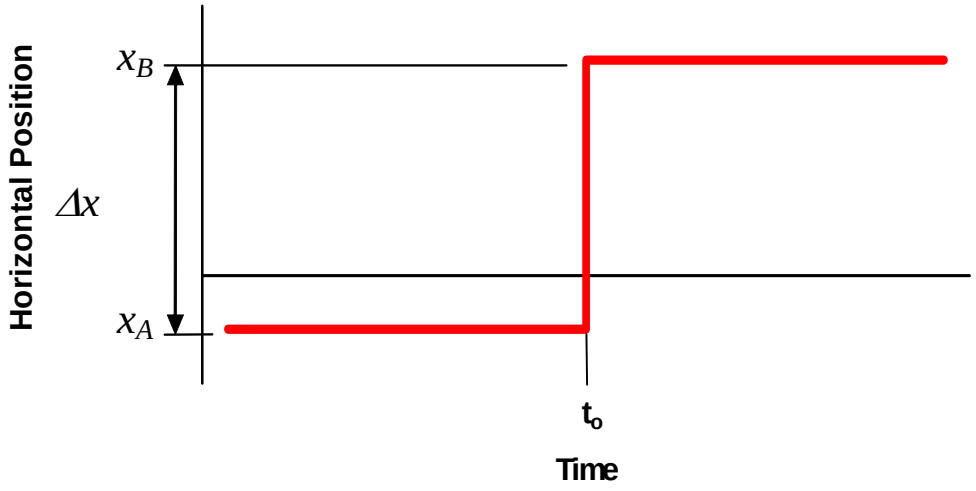

Figure 4.9: Simplified Displacement History

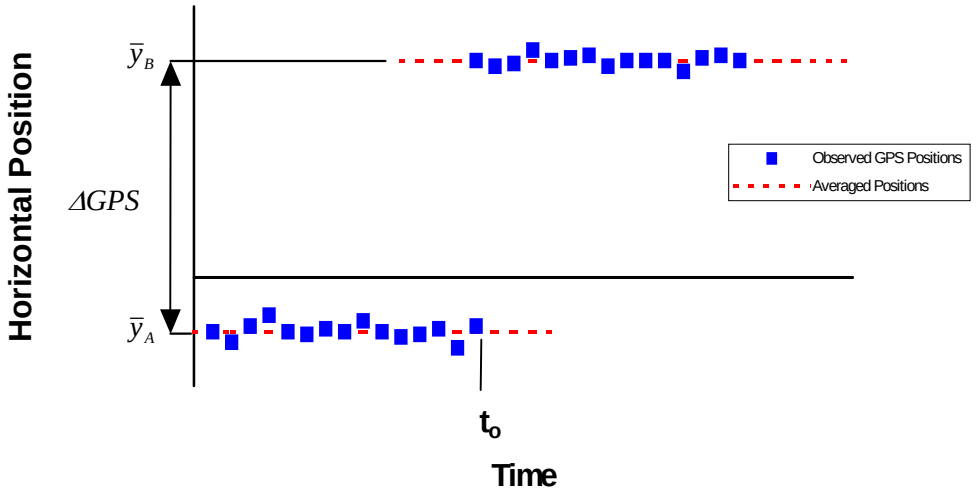

Figure 4.10: Sample Recorded Displacement History

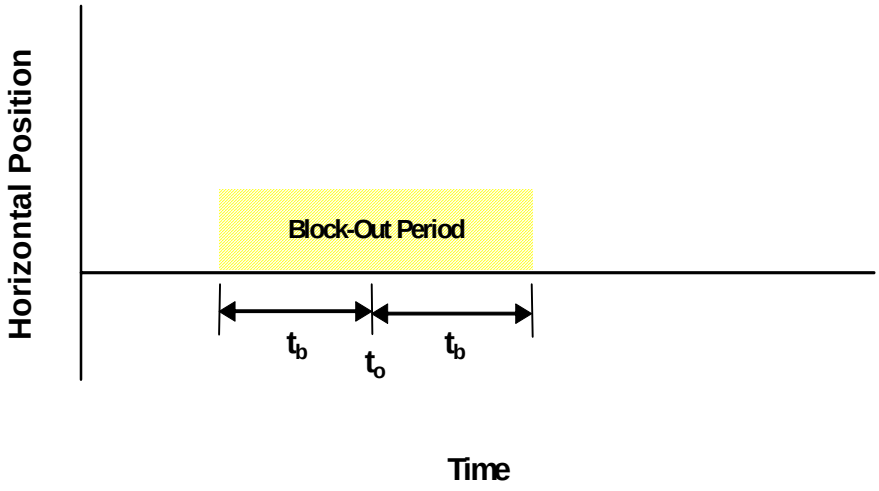

Figure 4.11: Data Block-out Period

In the analysis of the GPS data, amount of time used to determine the average values $\bar{y}_A$ and $\bar{y}_B$ was the primary parameter. This averaging duration is shown as Δt in Figure 4.12. Values between 1 min and 24 hr were considered for Δt. The maximum value for Δt for each analysis of GPS displacement depended on the length of time between consecutive station displacements.

In the following discussion, ΔGPS values will be calculated for each reference time, t_o, using various averaging durations, Δt. These data will be used to determine the minimum length of time over which the GPS data must be averaged to achieve a desired level of positioning accuracy.

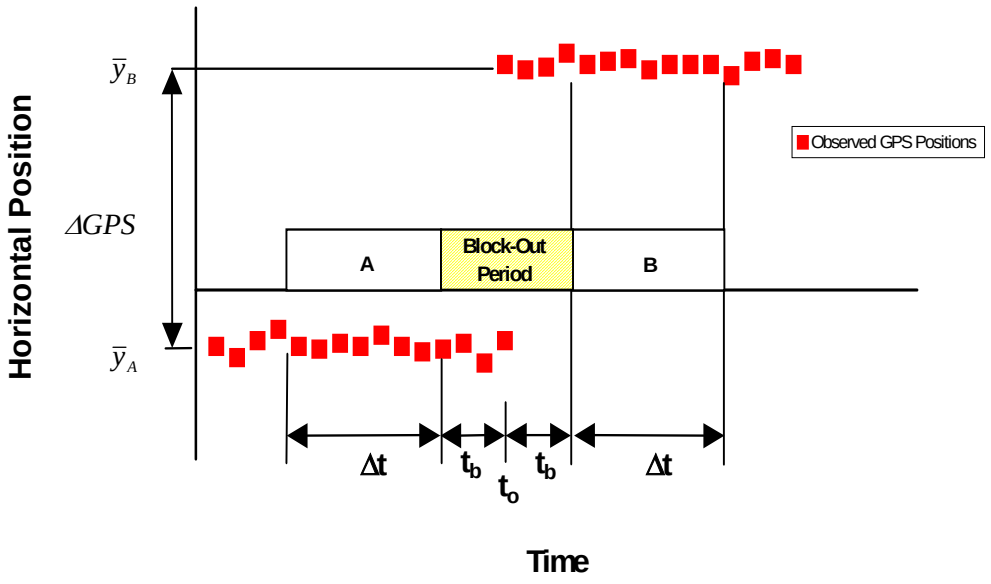

Figure 4.12: Data Averaging Periods

4.5 RESULTS OF HORIZONTAL TESTING

Testing of the NetForce GPS in the horizontal plane was divided into three phases: long-term static testing, short-term static testing, and dynamic testing. The long-term static test involved leaving the GPS stations in one position for a single five-week period. Short-term static testing involved moving each GPS station three times over a period of approximately one month. Finally, the dynamic testing phase involved seven discreet displacement histories, each imposed over a relatively short period of time. Each sequence of movements was intended to test the horizontal positioning accuracy of the GPS while simulating an actual bridge installation condition.

4.5.1 Long-Term Static Tests

Before imposing any displacement histories, both rover GPS units were left in stationary positions for five weeks. Data were recorded continuously throughout this period. The tests were originally designed to determine the background noise inherent to GPS readings, and thereby establish the horizontal accuracy of the NetForce system. However, the measured data indicated that the horizontal accuracy varied with the time of day as the number of satellites transmitting information to the GPS units changed.

(a) Evaluation of Data

More than 300,000 GPS readings were recorded by each rover unit during the long-term static tests. Clearly, the data must be organized into groups of manageable size in order to evaluate them carefully. As a first step, the data were grouped into five, one-week periods. Eight reference times, spaced at three-hour intervals, were then selected for each day. These reference times correspond to t_o in Figure 4.10, and were taken as 1 am, 4 am, 7 am, 10 am, 1 pm, 4 pm, 7 pm, and 10 pm (Central Standard Time) for each reference time, t_o, values of ΔGPS were calculated corresponding to eight averaging durations, Δt, which range from 5 min to 24 hr.

The data are presented in three different ways in this section. In order to investigate trends in the data related to the time of day, the seven values of ΔGPS calculated at the same reference time, t_o, with the same averaging duration, Δt, collected during a given week were averaged. These data are discussed in Section 4.5.1(b).

The variability of the data collected during a given day was evaluated by averaging the eight values of Δ*GPS* calculated using the same averaging duration, Δ*t*. These data are discussed in Section 4.5.1(c). The variability of the data during a given week was evaluated by averging the 56 values of Δ*GPS* (7 days times calculated using the same averaging duration, Δ*t)*. These data are discussed in Section 4.5.1(d).

(b) Sensitivity of GPS Data to Time of Day

Every location on earth experiences periods during the day when the satellite coverage is dense enough to provide reliable GPS data. Conversely, every location will also experience periods when the satellite coverage is poor, and the quality of the GPS data degrades. Because satellite coverage repeats with a period of 24 hours, 4 minutes, the variation of the quality of the data with the time of day should be similar on adjacent days (Angus 2002). However, when comparing data sets that were collected more than fifteen days apart, the offset of periods of poor satellite coverage will exceed one hour. Therefore, variations in data due to satellite coverage will be important for long-term monitoring applications.

Figure 4.13 plots the variability of the horizontal position as a function of the duration of averaging Δ*t*, for Station 2 during the first week of the long-term static test (21 Nov 02 through 27 Nov 02). Because the stations were not repositioned during the five-week period, the variation in the horizontal position is simply the average of the Δ*GPS* values corresponding to a given reference time, t_o, as shown in Figure 4.10.

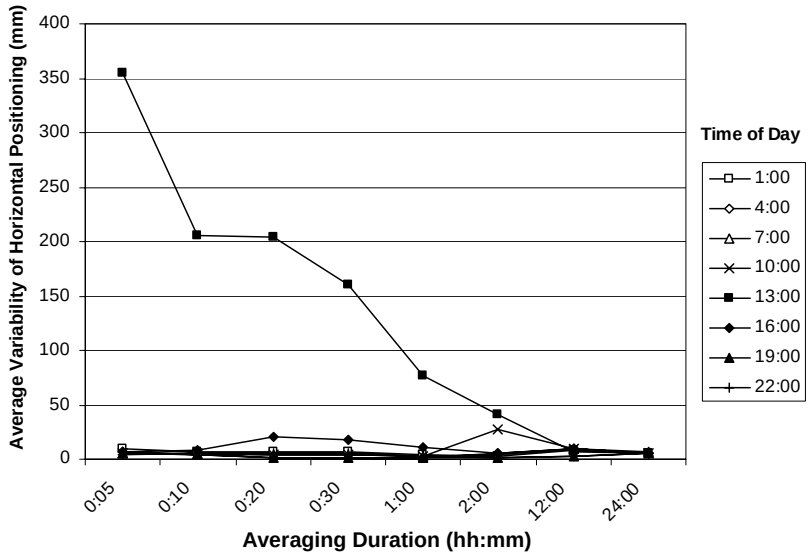

Figure 4.13: Variability of Horizontal Position with Time of Day (STA 2, Week 1)

A variation in the horizontal position of 0 mm would be ideal, indicating that the unit was stationary. As shown in Figure 4.14, the average variation was less than 10 mm for five of the eight reference times, t_o, and all averaging durations, Δ*t*. These data are consistent with the advertised "sub-centimeter" accuracy of the GPS monitoring system.

However, the variation in horizontal position of the data collected at a reference time of 13:00 exceeded 350 mm for the shortest averaging duration and exceeded 100 mm for all averaging durations less than 1 hr. This level of error is more than ten times the expected performance. The data corresponding to a reference time of 13:00 must be averaged for at least 12 hours before the level of noise is reduced to acceptable levels. The data corresponding to reference times of 10:00 and 16:00 experienced noise that exceeded 10 mm for several of the averaging durations.

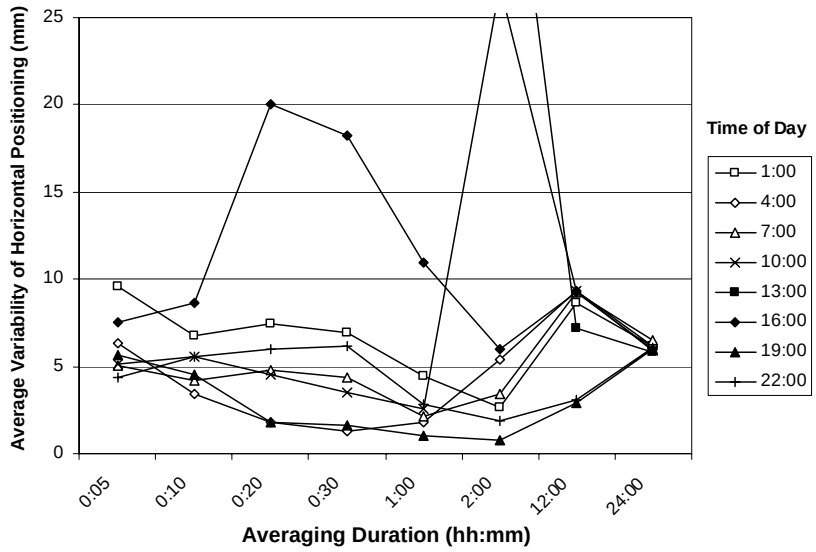

Figure 4.14: Variability of Horizontal Position with Time of Day (STA 2, Week 1) Expanded View

Similar data collected from Station 1 during the fifth week of the long-term static test (25 Dec 02 through 31 Dec 02) are plotted in Figures 4.15 and 4.16. The trends in the data are similar to those discussed, but the errors corresponding to a reference time of 13:00 decreased and those corresponding to a reference time of 10:00 increased. These changes can be explained by considering the satellite patterns over central Texas during the long-term static test. The variation in the number of satellites in view as a function of the time of day is plotted in Figures 4.17 and 4.18. This information was calculated using the approximate latitude and longitude coordinates of the GPS stations and known satellite patterns (A. Bilich 2003).

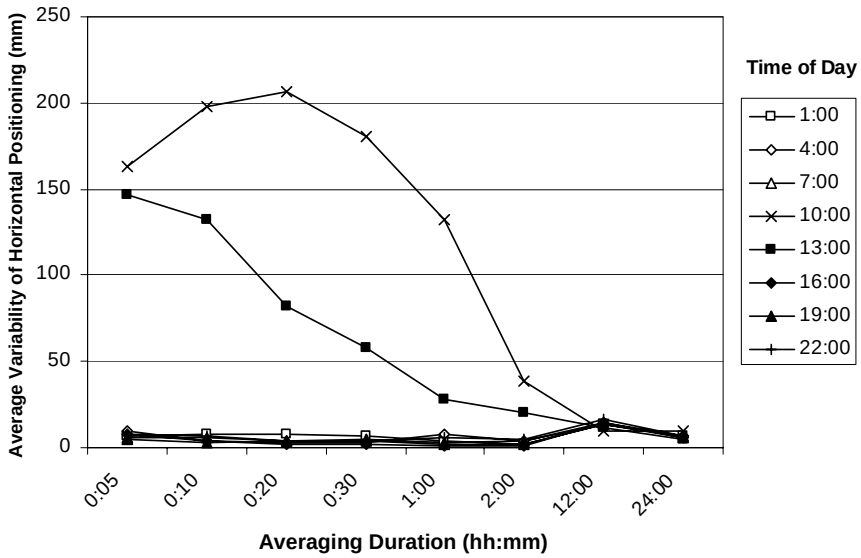

Figure 4.15: Variablility of Horizontal Position with Time of Day (STA 1, Week 5)

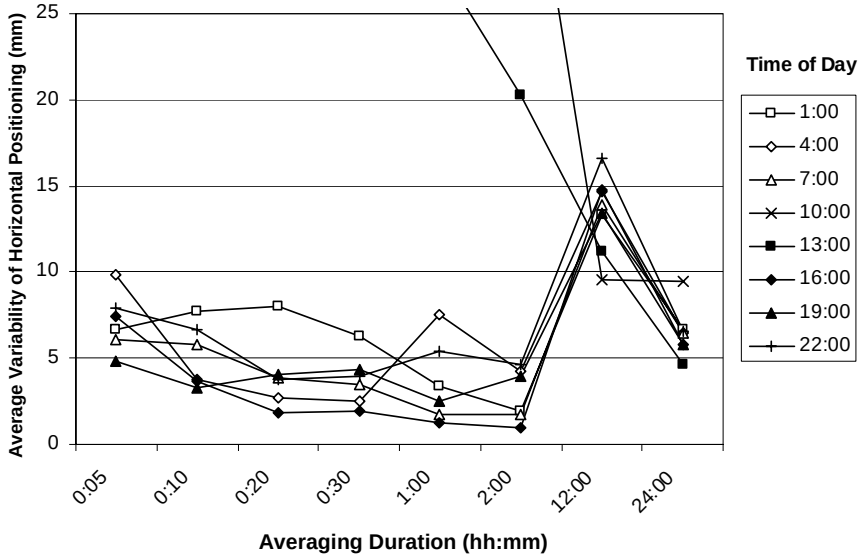

Figure 4.16: Variablility of Horizontal Position with Time of Day (STA 1, Week 5) – Expanded View

In order to obtain the most basic GPS solution, four satellites must be in view of a particular GPS station. The accuracy of the GPS solution increases with the number of satellites. Given the constellation of 24 satellites, distributed approximately equidistantly around the earth, a maximum of 12 satellites may be in view of a location at a given time.

Figure 4.17 shows that on Nov 21 02, satellite coverage was poor (5 satellites in view) for an extended period of time around 13:00, and for a very short time at 16:00. At other times, coverage was much better. As many as 11 satellites were in view at 06:00, but coverage remained high for the duration of the day. This distribution of satellites supports the data shown in Figure 4.13 for the same date.

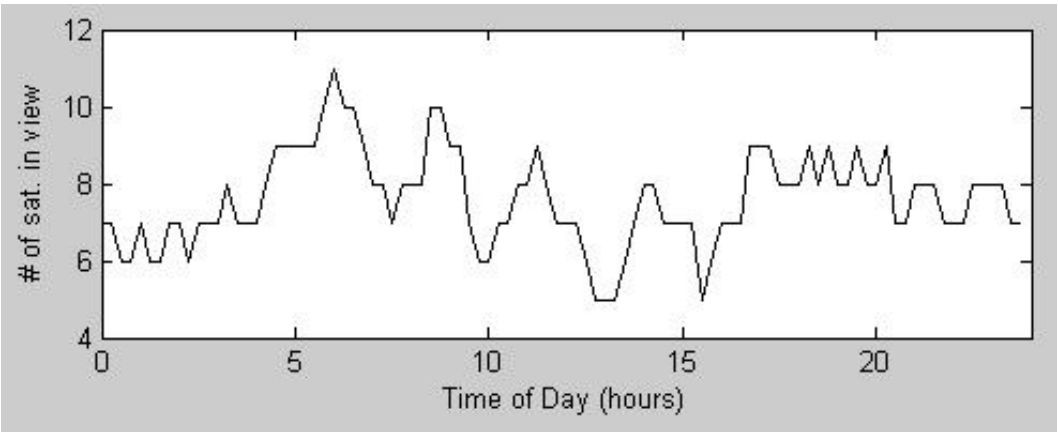

Figure 4.17: Number of Satellites Over Central Texas (21 Nov 02)

Figure 4.18 shows that on 27 Dec 02, satellite coverage was poor around 10:00 and 13:00. At other times of day, satellite coverage was better, allowing for good GPS solutions. Again, the distribution of satellites supports the data shown in Figure 4.15.

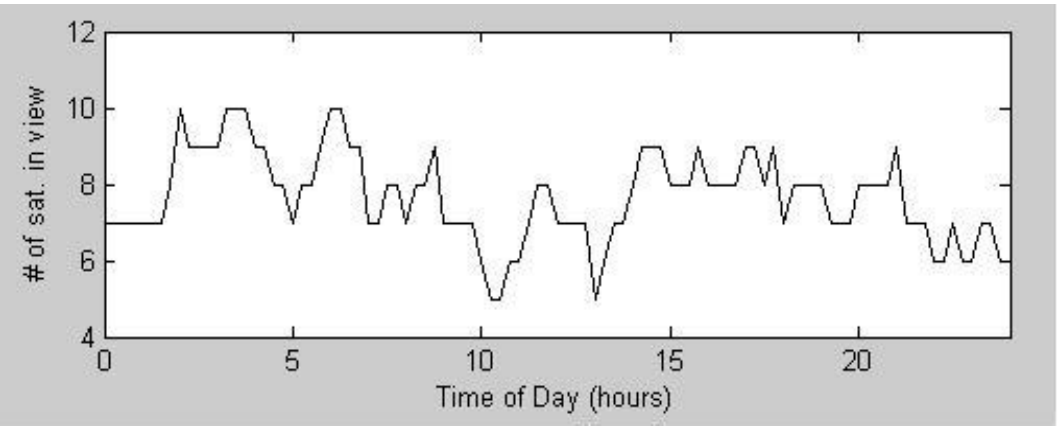

Figure 4.18: Number of Satellites Over Central Texas (27 Dec 02)

Every location on the surface of the earth will experience this type of variation in satellite coverage. However, the times of maximum and minimum satellite coverage will vary. Although the variations in satellite coverage cannot be avoided, this information must be considered when interpreting GPS data.

(c) Daily Averages

Figures 4.19 and 4.20 represent plots of the average error, ΔGPS, corresponding to a given averaging duration, Δt, for seven, 24-hr periods. Data from each of the eight reference time are included in these plots of daily averages.

The observed data are highly variable. During the second week of the long-term static tests, the errors were consistently low. The maximum average error was less than 20 mm. In contrast, the average error exceeded 100 mm for averaging durations of 1 hr and less during the first day of the fifth week of the test.

(d) Weekly Averages

When all 56 values of ΔGPS corresponding to a given averaging duration, Δt, collected during one week are averaged, the anomalies observed in the daily averages are not as noticeable. Figure 4.21 shows data from each week of the long-term static test collected by Station 2.

The average errors for 5-min averaging durations ranged from 49 mm in Week 1 to 10 mm in Week 5. As the averaging durations increased, the errors tended to drop. The weekly average error was less than 15 mm for an averaging duration of 12 hr and was approximately 5 mm for an averaging duration of 24 hr.

The same data are plotted in Figure 4.22, but the values of ΔGPS corresponding to a reference time of 13:00 were not considered in the analysis. The average error is reduced dramatically for the shorter averaging durations. The average error was approximately the same for averaging durations of 12 and 24 hr.

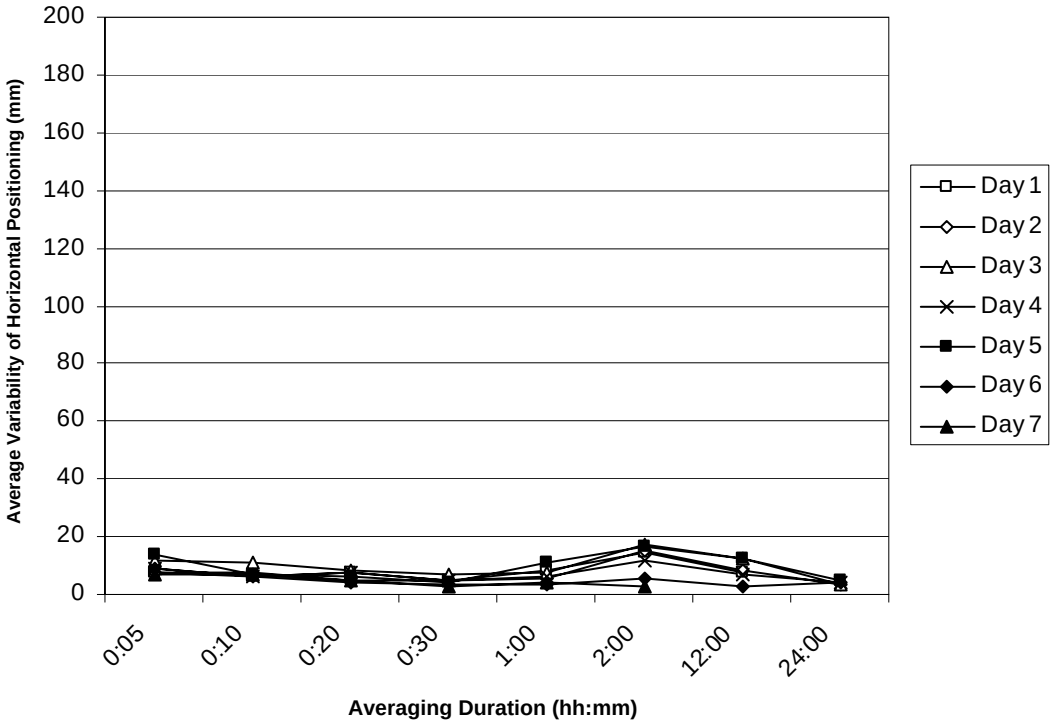

Figure 4.19: Daily Average of Variation in Horizontal Position (STA 2, Week 2)

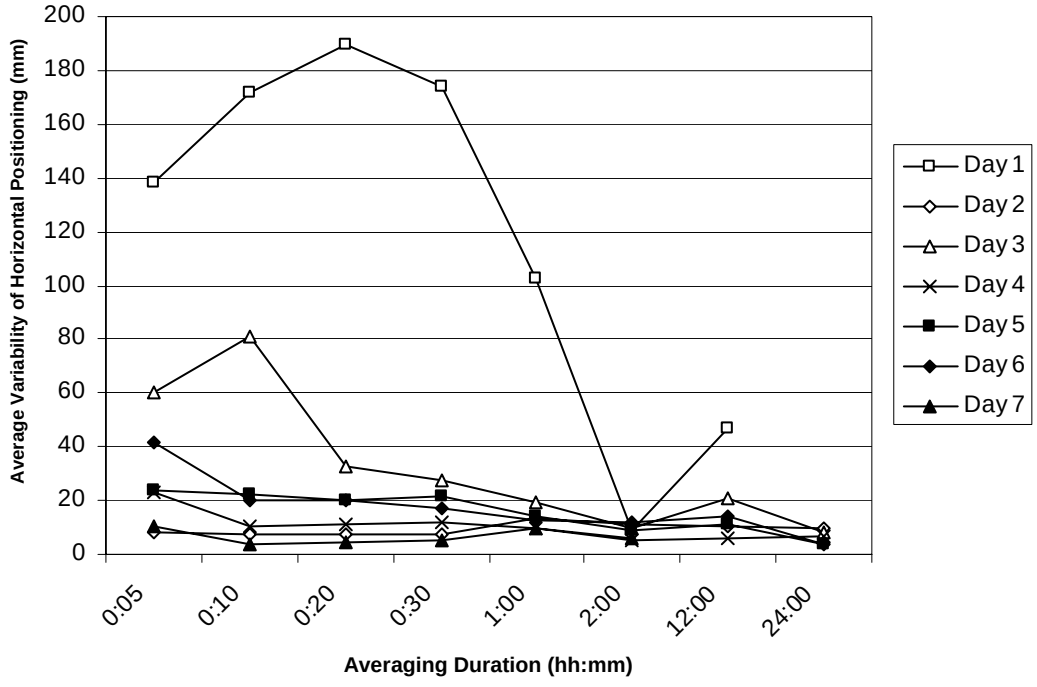

Figure 4.20: Daily Average of Variation in Horizontal Position (STA 1, Week 5)

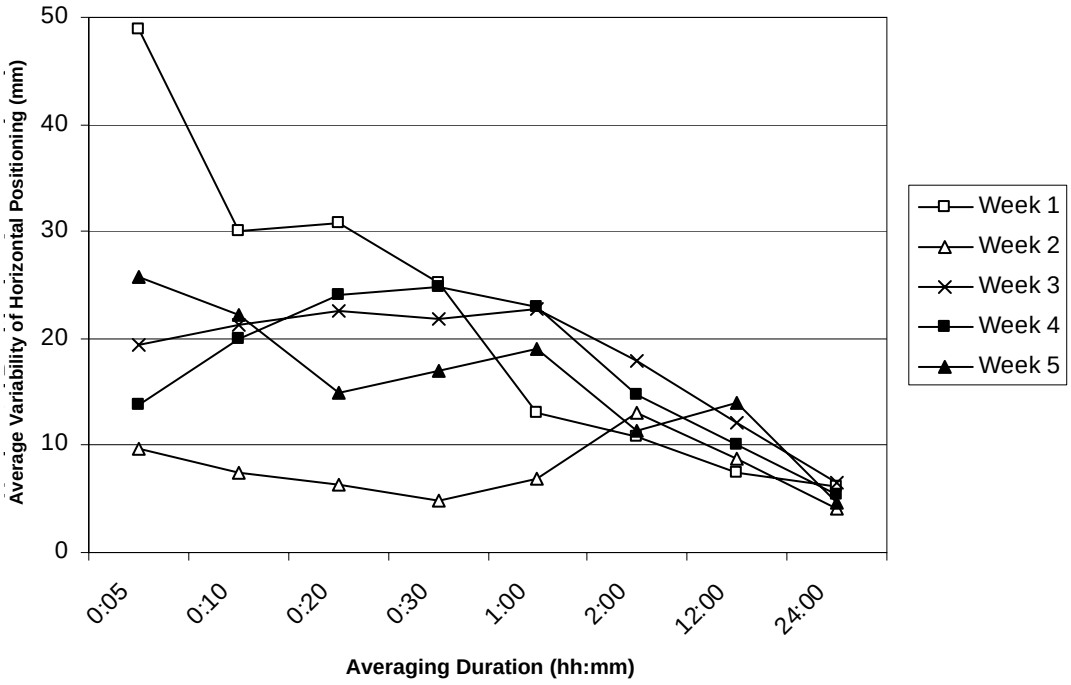

Figure 4.21: Weekly Averages of Variation of Horizontal Position (STA 2)

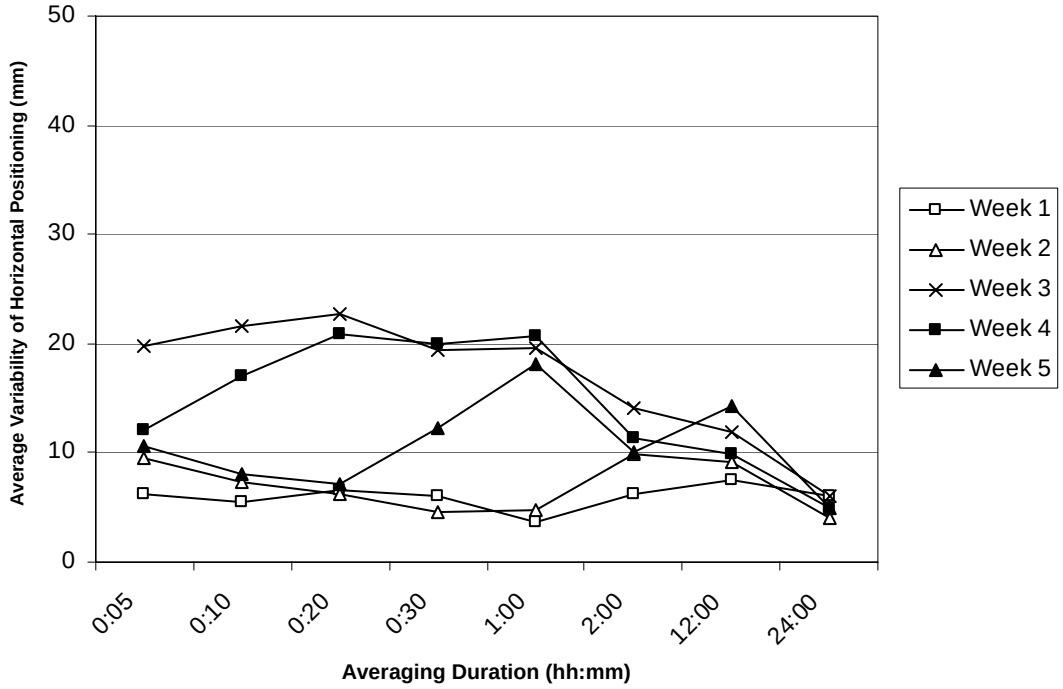

Figure 4.22: Weekly Averages of Variation in Horizontal Position – Data with a Reference Time of 13:00 Not Considered (STA 2)

4.5.2 Short-Term Static Tests

During the short-term static tests, the GPS units were moved from Position x_A to Position x_B at time t_o (Figure 4.9). The unit was then stationary for several days (Table 4.2). The measured GPS data are compared with the known displacement histories in this section.

(a) Evaluation of Data

The variation in the GPS data, ΔGPS, was calculated using eight averaging durations, Δt, for the short-term static tests. The data are presented in Tables 4.3 and 4.4. Unlike the long-term static tests, the values of ΔGPS were not averaged in the test series.

(b) Observations

Five of the six short-term static tests yielded expected levels of error. Placement errors were typically less than 20 mm when the averaging duration was 10 min or more. However, the error levels were extremely large during the second test of STA 2. The error during this test was more than 450 mm for an averaging duration of 5 mm. In contrast, the error was 0.1 mm for the third test of STA 2.

The results of the short-term static tests indicated that error levels can vary significantly for nominally identical tests conducted simultaneously.

Table 4.2: Characteristics of Short-Term Static Tests

Movement Sequence	Horizontal Displacements STA 1 (mm)	Horizontal Displacements STA 2 (mm)	Date of Movement	Time of Movement (hh:mm)
1	120.0	100.0	1 Oct 02	16:00
2	123.7	104.4	8 Oct 02	15:50
3	28.3	28.3	10 Oct 02	20:30

Table 4.3: Results from Short-Term Static Tests (STA 1)

Actual Displacement (mm)	Observed Displacements (mm)							
	5 min	10 min	20 min	30 min	1 hr	2 hr	12 hr	24 hr
120.0	105.4	102.4	84.9	76.2	95.0	92.6	113.4	111.8
123.7	131.7	120.4	155.5	158.0	140.4	117.1	119.6	120.5
28.3	25.7	25.7	26.9	27.2	27.4	26.9	31.8	24.9

Table 4.4: Results from Short-Term Static Tests (STA 2)

Actual Displacement (mm)	Observed Displacements (mm)							
	5 min	10 min	20 min	30 min	1 hr	2 hr	12 hr	24 hr
100.0	74.9	108.3	101.7	100.2	94.6	98.4	99.3	96.7
104.4	576.1	557.1	572.0	411.6	248.1	172.1	115.5	109.1
28.3	28.4	28.9	29.7	28.9	31.0	29.2	23.4	25.2

4.5.3 Dynamic Tests

During the last series of tests to evaluate the horizontal accuracy of the GPS systems. The rover stations were subjected to predefined displacement histories (Table 4.5). A total of seven displacement histories were defined, and during each test the GPS stations were moved by a displacement increment at a constant time interval. The time intervals varied from 30 min to 1 day and the displacement increments varied from 1 to 40 mm. In some tests, the units were moved in the same direction and by increments of the same amplitude each time. In other tests, the direction of movements was varied, but the amplitude of the displacement increment was constant. Both the amplitude of the displacement increment and the direction were varied in other tests. This variety of displacement histories was intended to duplicate the variety of movements that a bridge may experience due to daily temperature fluctuations or structural degradation with time.

Data from all the dynamic tests are discussed in the thesis by Bilich (2003). Only data from displacement histories 4 and 8 are discussed in this report. GPS positions recorded at STA 1 are plotted as a function of time in Figures 4.23 and 4.24. Calculated values of ΔGPS are also summarized in Tables 4.6 and 4.7 for a variety of averaging durations, Δt.

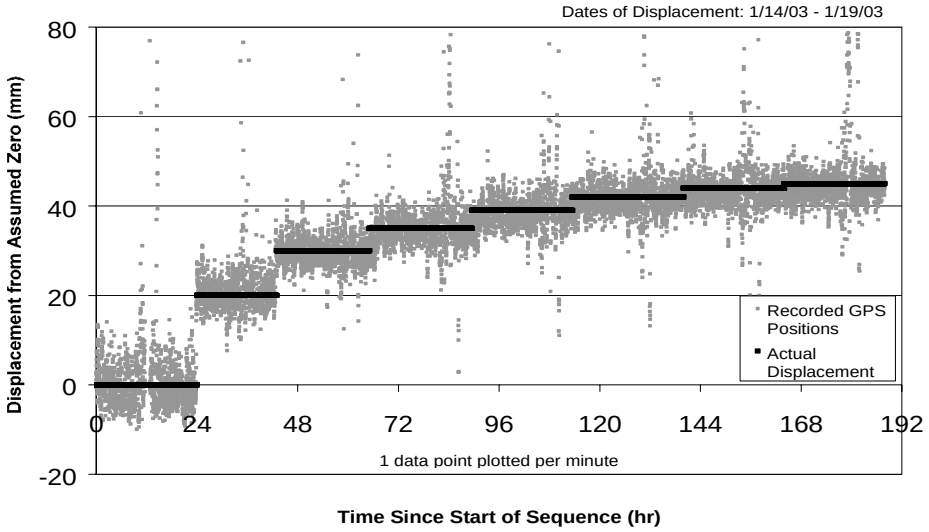

Figure 4.23: Dynamic Test 4 (STA 1)

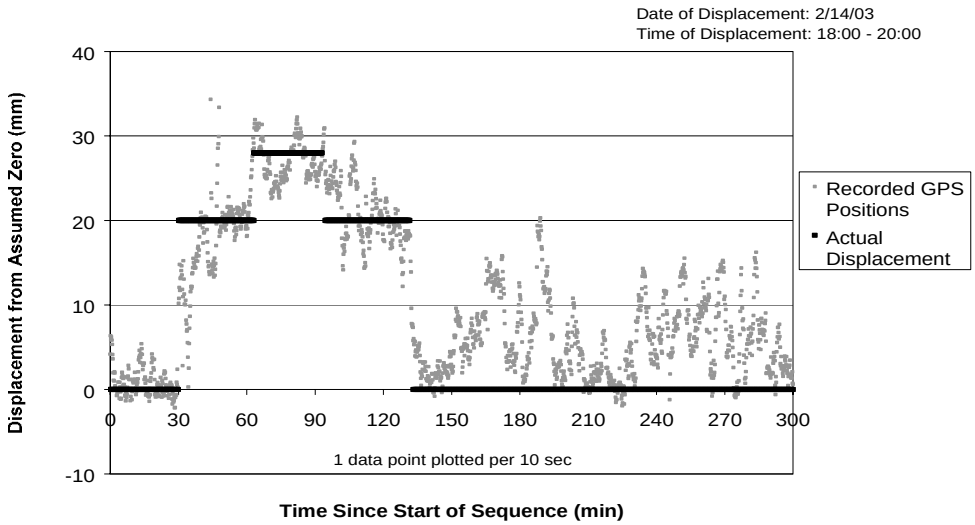

Figure 4.24: Dynamic Test 8 (STA 1)

Table 4.5: Dynamic Tests

Displacement History	Horizontal Displacement Increment N+/S- (mm)	W+/E- (mm)	Duration of Each Displacement (hr) Increment
4	0	+20	24
	0	+10	
	0	+5	
	0	+4	
	0	+3	
	0	+2	
	0	+1	
5	0	+10	0.5
	0	+10	
	0	+10	
	0	+10	
	0	+10	
	0	+10	
	0	+10	
	0	+10	
6	0	+10	1
	+10	0	
	0	+10	
	+10	0	
7	0	-20	2
	0	-20	
	0	-20	
	0	-20	
8	+20	0	0.5
	0	-20	
	-20	0	
	0	+20	
9	+40	0	1
	0	-40	
	-40	0	
	0	+40	
10	-40	0	2
	0	-40	
	+40	0	
	0	+40	

Displacement history 4 was designed to evaluate the sensitivity of the GPS data. As the amplitude of the displacement increment decreases, the change between successive positions approaches the baseline noise level. Although the GPS data were recorded every 10 sec, every sixth point is plotted in Figure 4.23, yielding one data point per minute. A total of eight positions, each held for 24 hr, comprised the sequence. The data recorded during the first interval were averaged to obtain a baseline for the entire test. Changes in GPS position were plotted relative to this baseline.

As the displacement increments were induced, the GPS data tended to cluster about the actual position of the station, and the GPS data during each time interval tends to be centered about these positions. When the displacement increments fell below 3 to 4 mm, the data began to blend together and distinctions between displacement intervals were not obvious. This trend suggests an accuracy plateau in the GPS data.

Times of particularly high error were noticed during each of the eight 24-hr periods. These periods are indicated in the figures by the large deviations from the expected values and occurred approximately 18 hr from the beginning of each 24-hr displacement increment. These times range from 10:00-11:00 am corresponding to times when satellite coverage is lowest over the test site during the week of testing, 14 Jan 03 through 21 Jan 03. Although not shown on the plots, errors as large as 2,035 mm were observed during the sequence, when the data recorded every 10 sec were considered.

With 24-hr averaging durations, it is possible to reduce the effects of these data anomalies and resolve displacement increments as small as 3 or 4 mm. It was not possible to resolve displacement increments smaller than these values.

Displacement history 8 was designed to evaluate the ability of the GPS system to detect a simple movement pattern and return to the original position. The displacement increments were imposed at approximately 30-min intervals. The data recorded during the first 30-min interval was averaged and served as the baseline for the entire displacement history. The data are plotted in Figure 4.24 and summarized in Table 4.7 for averaging durations between 5 min and 30 min.

Because of the nature of the raw GPS data provided to the research team by Mezure, it was not possible to resolve each movement into east/west and north/south components. The vector distance of the station from the starting point of the displacement sequence was the only available measurement. The maximum vector displacement value during the 20-mm square displacement sequence occurred when the station was at the corner opposite the starting point. This maximum displacement value was 28.3 mm.

The recorded GPS positions in dynamic test 8 exhibited reasonable clustering around the actual positions when the stations were displaced. Normal variability was observed in the individual GPS positions. Most data points were within 10 mm of the actual displacement at any time. No large-displacement variabilities were observed during this displacement sequence. However, satellite coverage was acceptable during this entire test.

After the displacement history was completed and the GPS stations returned to the initial positions, recorded GPS positions were 5 to 10 mm above the baseline zero. This depicts the random nature of unaveraged GPS positions taken over a brief period of time, such as the 30-min intervals. Although 30 min of data were averaged to obtain a zero-displacement reference value, the GPS environment (satellite coverage, atmospheric conditions, etc.) had changed by the conclusion of the 90-min test. Rapid GPS movements can be sensed relatively quickly, but the true position cannot be calculated without sufficient averaging time.

Table 4.6: Average GPS Data from Dynamic Test 4 (STA 1)

Actual Displacement (mm)		Average Displacement (mm)							
N+/S-	W+/E-	5 min	10 min	20 min	30 min	1 hr	2 hr	12 hr	24 hr
0	+20	10.0	12.7	14.9	16.7	18.1	19.6	27.9	25.7
0	+10	1.9	8.4	9.0	9.5	9.5	10.1	14.4	16.4
0	+5	7.7	11.4	7.7	5.2	5.1	5.5	5.1	5.0
0	+4	8.4	6.4	5.7	5.3	5.6	5.7	5.9	2.7
0	+3	7.6	5.2	3.8	2.6	3.0	3.4	8.4	3.9
0	+2	4.9	8.8	5.8	1.7	1.2	3.2	5.1	9.3
0	+1	4.6	5.7	1.6	3.2	2.3	2.0	2.1	4.9

Table 4.7: Average GPS Data from Dynamic Test 8 (STA 1)

Actual Displacements (mm)		Average Displacement (mm)			
N+/S-	W+/E-	5 min	10 min	20 min	30 min
+20	0	19.9	18.4	21.7	19.0
0	-20	19.2	17.5	17.9	19.5
-20	0	19.1	20.1	22.1	22.1
0	+20	20.2	21.6	21.0	20.3
	Average	**19.6**	**19.4**	**20.7**	**20.2**
	Closing Values	9.2	9.4	12.2	13.3

4.5.4 General Observations

In general, the measured GPS data achieved sub-centimeter accuracy levels when the data were averaged 12 to 24 hr. However, disturbances in the data were observed. Evidence of increased error associated with loss of satellite coverage was observed during the long-term static and dynamic tests. Significant variations in the errors recorded during successive weeks were also observed, but the source of these errors was not identified.

When the incremental displacements were less than 3 to 4 mm, background noise inherent to the reported GPS positions tended to dominate the response. Smaller displacement increments could not be detected from the GPS data.

Increasing the averaging duration tended to improve the positioning accuracy, but only up to this level of 3 to 4 mm. In some tests, 24-hr averaging periods successfully resolved displacements less than 3 to 4 mm in magnitude. However, this behavior was not representative of the system behavior. It is possible that

averaging durations greater than 24 hr could resolve displacements smaller than the plateau value. This research, however, did not average values over durations greater than 24 hr.

Closing values for box displacement sequences were quite erratic in nature and lacked the accuracy present in other measurements. When the stations were returned to the initial position, residual displacement values ranged from 3 to 13 mm. Although some of the most accurate values were generated with 2 hr of averaging durations of 2 hr, others were generated with only 5 min of averaging duration. This unpredictable closing behavior was likely caused by changing GPS conditions and may have been aided by increased averaging durations.

4.5.5 Alternative Evaluation of Data

This section discusses an alternative method for analyzing the GPS data. Rather than comparing blocks of averaged data before and after each reference time, t_o, to obtain a relative displacement between the two blocks, data acquired immediately prior to each reference time were averaged and compared with an assumed baseline value as shown in Figure 4.25. Additional averaging durations were used in this method, with values ranging from 10 min to 24 hr. The resulting plots yielded a smoother relationship between horizontal accuracy and averaging durations than in the previous analysis.

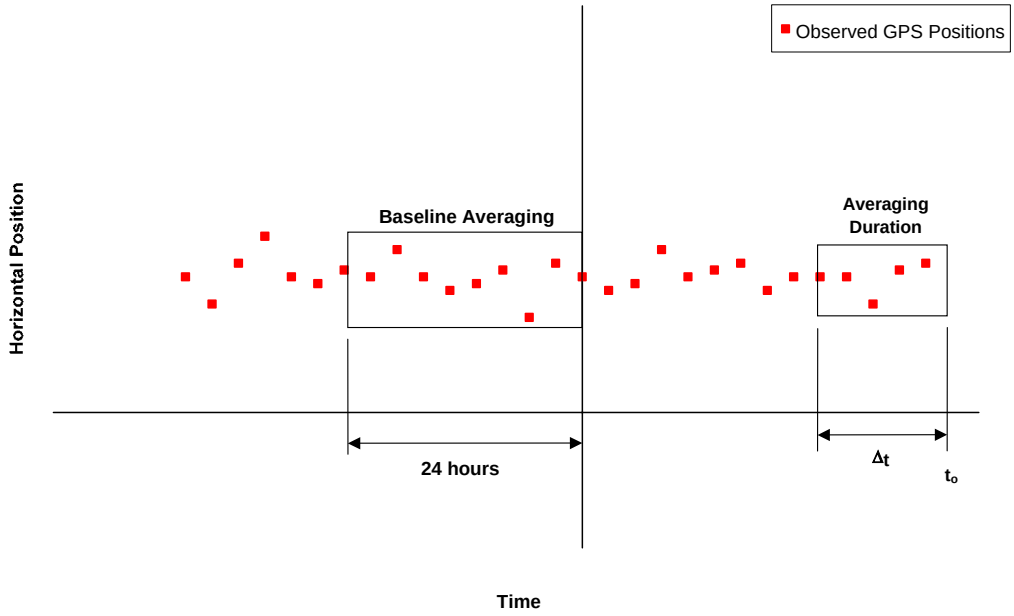

Figure 4.25: Alternative Analysis Method

The baseline positions for this analysis were obtained by averaging GPS data for 24 hr. Because all displacement data were compared with the same baseline value, the duration used to obtain the baseline value is relatively unimportant. The change in the relative displacements calculated for each averaging duration was the variable of interest.

The data acquired during Week 1 of the long-term static tests were analyzed using this alternative technique. The variability of the horizontal position with the time of day is shown in Figure 4.26 for averaging durations between 1 hr and 24 hr. The same raw data were used to generate Figures 4.13 and 4.26 but interesting trends in the data are more apparent in Figure 4.26. As discussed in Section 4.5.1, reduced satellite coverage was observed during the first week of the long-term static test at a reference time, t_o, of 13:00. The data in Figure 4.26 support this observation. Data averaged immediately before

13:00 exhibit errors approaching 400 mm (not shown in Figure 4.26). As the averaging duration increases, the limiting accuracy of the system is seen to be 6 mm for STA 2. This value is consistent with the results discussed in earlier sections.

As the reference time, t_o, moves further from 13:00, the overall accuracy of the data improves. However, when the averaging duration, Δt, is long enough to include data from 13:00, the errors increase dramatically.

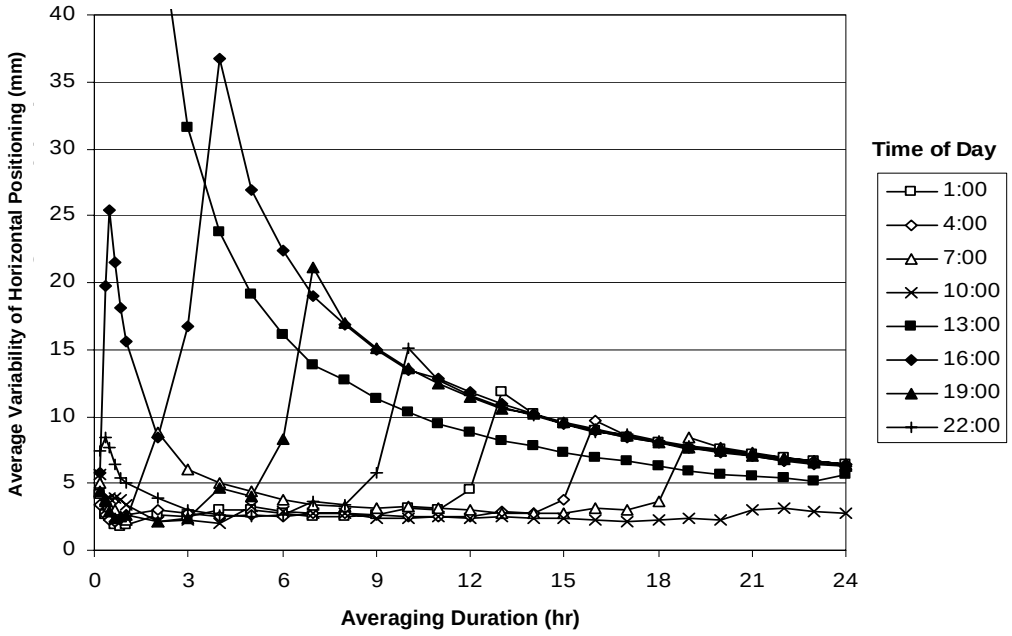

Figure 4.26: Alternate Presentation of Variability of Horizontal Position with Time of Day (STA 2, Week 1)

Once data from 13:00 are included in the average, it becomes a challenge for the system to remove this error through averaging within a 24-hr period. Although short-term accuracy is very good at some times of the day, the accuracy of the system on the whole is depicted by the behavior at the end of the curve, as averaging durations approach 24 hr. The accuracy plateau when averaging over 24 hr is found to be approximately 5 mm.

4.5.6 Conclusion

The NetForce global positioning system generally performed at or better than the advertised sub-centimeter level of accuracy in a variety of dynamic testing environments. These tests showed that increased averaging durations did improve system accuracy up to a threshold of 3 to 4 mm. Satellite coverage had a significant influence on the observed errors.

4.6 RESULTS OF VERTICAL TESTS

Similarly to the horizontal tests described in Section 4.5, a series of tests was developed to evaluate the sensitivity of the GPS data to vertical displacement. These tests are described in this section.

4.6.1 Vertical Displacement Histories

Each GPS station was subjected to seven displacement histories, which are summarized in Table 4.8.

Table 4.8: Vertical Displacement Histories

Displacement History	Vertical Displacements STA 1 Up + / Down – (mm)	Vertical Displacements STA 2 Up + / Down – (mm)	Duration of Each Displacement Increment
1	+19.1	+19.1	3 days
2	+18.9	+19.3	17 days
3	+6.6	+6.6	7 days
4	-6.5	-6.5	1 hour
4	-6.4	-6.6	1 hour
4	-6.4	-6.3	1 hour
4	-6.3	-6.5	1 hour
4	-6.4	-6.4	1 hour
5	-12.7	-12.8	13 days
6	+2.6	+2.6	4 days

Displacement history 4 was the only test that contained short displacement increments. This sequence was intended to replicate a structure experiencing rapid vertical movement. In this case, the structure would be sinking at a rate of approximately 6 mm per hour.

4.6.2 Data Recovery Issues

Immediately following the final vertical test on 14 Apr 03, attempts were made to contact Mezure, Inc., requesting transfer of the final GPS data set. This data set contained the vertical displacement data for all seven displacement histories. Over the next month, Mezure did not answer telephone calls or return e-mail messages. As of 1 May 03, the MezureNet website as well as the company homepage, were no long accessible over the internet.

The research team was never able to contact Mezure to obtain the data from the vertical tests. The 2003 second quarter financial report for NovAtel lists Mezure as a "discontinued operation." NovAtel held a 70% equity interest in Mezure at the time. The GPS units were returned to NovAtel in Dec 03.

This experience highlights the importance of evaluating the financial stability of any company before entering a long-term contract for bridge monitoring.

CHAPTER 5:
CONCLUSIONS AND RECOMMENDATIONS

The goal of this research was to provide options for use by TxDOT to monitor the structural health of unique bridges in Texas. Two proprietary data acquisition systems were selected for testing and evaluation in satisfying these goals. The first system discussed was an autonomous data acquisition system for strain called *MicroSAFE*. The second system discussed was a global positioning system called *NetForce*.

5.1 CONCLUSIONS

Both technologies discussed in this report are viable for use by TxDOT. Each system is user-friendly, providing immediate return of meaningful engineering data with minimal effort on the part of TxDOT.

The MicroSAFE system can record raw strain data and compute rainflow counts for use in fatigue analysis of structural components. The system is compact, inexpensive, and simple to use. As areas of interest are identified during routine inspections, a single TxDOT inspector can install the system and program it to acquire rainflow data in a matter of minutes. When data acquisition is complete, rainflow data acquired over consecutive 24-hr periods show how the structural component is performing under service loads and the likelihood of fatigue damage can be immediately assessed. As a result, important questions regarding the condition of the structure can be answered in a very short period of time, and with a minimum of effort on the part of the engineer or inspector.

The NetForce system measures long-term variations in structural displacements. In most cases, the system achieved and error threshold of 3 to 4 mm. Once the system hardware is purchased, it will be installed, monitored, and maintained by Mezure personnel. Both current and previous displacement data will be available at any time via a secure website. Large amplitude displacements will trigger preset alarms and alert TxDOT personnel.

5.2 CAVEATS

Based on the tests described in this thesis, the research team cautions that short-term GPS data may be unreliable due to daily fluctuations in the satellite coverage. Only displacement values averaged over time will generate stable and reliable information using a GPS-based system. As a result, data should be averaged for 24 or more hours before making any conclusions. This may limit the possible applications of the GPS-based system.

Also, when selecting a system that will be maintained and monitored by an outside firm for a long duration, the purchaser of the system must evaluate the financial stability of that firm before entering a long-term contract for services. The research team lost contact with Mezure when operations were discontinued in June 03.

5.3 FUTURE WORK

The monitoring technologies described in this thesis appear to meet the objectives established for structural health monitoring. Field testing will be implemented in the next stage of this project.

REFERENCES

Alampalli, S. (1995). *Measuring Bridge Vibration for Detection of Structural Damage*. New York Department of Transportation.

Alampalli, S. (1999). "Significance of Operating Environment in Condition Monitoring of Large Civil Structures. Shock and Vibration," Vol. 6, No. 5, pp. 247-251.

American Institute of Steel Construction (1998). *Manual of Steel Construction: Load & Resistance Factor Design.* AISC, Inc. 1998.

Angus, M. (2001). *E-mail conversation with Mezure staff regarding Florida DOT participation.*

Angus, M. (2002). *E-mail conversation with Mezure staff.*

ASTM E 1049 (1997). *Standard Practices for Cycle Counting in Fatigue Analysis.* American Society for Testing and Materials.

Bilich, A.L. (2003). *Matlab script for generating plots of number of satellites over a specific location.*

Bilich, A.L., et. al. (2002). *SNR-based Multipath Corrections to GPS Phase Measurements.* PowerPoint presentation. University of Colorado – Boulder.

Bilich, C.T. (2003). *Evaluation of Two Monitoring Systems for Significant Bridges in Texas*, M.S. Thesis, Department of Civil Engineering, University of Texas at Austin.

Buhl, M. (2003). *Crunch – A batch-oriented Postprocessor for Wind Turbine Data Analysis*. http://wind.nrel.gov/designcodes/crunch/, National Wind Technology Center.

Conner, G. and Conway, F. (2001). *E-mail conversation with Alabama DOT personnel*.

Downing, S.D., and Socie, D.F. (1982). "Simplified Rainflow Counting Algorithms," *International Journal of Fatigue*, Vol. 4, No. 1, pp. 31-40.

Duff, K. and Hyzak, M. (1997). *Structural Monitoring with GPS*. *Public Roads*, 1997. http://www.tfhrc.gov/pubrds/spring97/gps.htm

Frank, K.H. (2003). *CE 397 – Experimental Techniques*. Class Notes.

Givan, G. (2001). *E-mail conversation with Kentucky DOT personnel*.

Haigood, A. (2002). *E-mail conversation with Invocon staff.*

Hofmann-Wellenhof, B., Lichtenegger, H., and Collins J. (1997). *Global Positioning System: Theory and Practice*, Fourth Ed., Springer Wien, New York.

Palmgren Steel Products Manual for Milling Table (PN 49181).

Misra, P. and Enge, P. (2001). *Global Positioning System: Signals, Measurements, and Performance*, Ganga-Jamuna Press. Lincoln, Massachusetts.

National Academy of Sciences (1995). *The Global Positioning System.* National Academy Press. Washington, D.C.

National Instruments (2003). *Document on Data Aliasing*.

Neislony, A. (2003). *Rainflow Counting Method*. (Matlab computer program), http://www.mathworks.com

O'Shea, D. (2001). *E-mail conversation with Delaware DOT personnel*.

Scott, J.S. (1984). *The Penguin Dictionary of Civil Engineering*. Penguin Books, Ltd.

Sime, J. and D'Attilio, P. (2001). *E-mail conversation with Connecticut DOT personnel*.

TexasFreeway.com (2003). http://www.texasfreeway.com

Vishay, Inc. (2003). http://www.vishay.com